Applied Mathematical Modelling 118 (2023) 618–640

Contents lists available at ScienceDirect

Applied Mathematical Modelling

journal homepage: www.elsevier.com/locate/apm

Event-triggered extended dissipativity stabilization of semi-Markov switching systems

Wenhuang Wu[a], Ling He[a], Zhilian Yan[b], Jianping Zhou[a,*]

[a] School of Computer Science & Technology, Anhui University of Technology, Ma'anshan, 243032, Anhui, China
[b] School of Electrical & Information Engineering, Anhui University of Technology, Ma'anshan, 243032, Anhui, China

ARTICLE INFO

Article history:
Received 21 May 2022
Revised 30 January 2023
Accepted 31 January 2023
Available online 7 February 2023

Keywords:
Semi-Markov switching system
Stochastic stability
Event-triggered control
Extended dissipativity

ABSTRACT

This paper is concerned with event-triggered extended dissipativity stabilization of uncertain semi-Markov switching systems with external disturbances. The purpose is to ensure the stochastic stability and extended dissipativity of the semi-Markov switching systems via using event-triggered control. A mode- and disturbance-dependent switched event-triggered mechanism is devised to determine the triggered moments, which can further reduce the number of triggered events compared to some existing switched event-triggered mechanisms. On the basis of the proposed mechanism, a time- and mode-dependent piecewise-defined Lyapunov functional is constructed to establish a criterion for the stochastic stability and extended dissipativity. Subsequently, a co-design scheme for the needed feedback-gain and event-triggered matrices is presented using some equivalent transformations of matrix inequalities. Lastly, a DC motor model and a robotic arm model are utilized to illustrate the validity of the designed controller.

1. Introduction

Random behaviors, such as failures and repairs of components, as well as interconnection variations, may result in abrupt changes in the structure or parameters of a control system [1]. In order to describe, explain, predict and control state evolution trends of this class of systems, various Markov switching systems (MSSs) modeled by linear or nonlinear differential equations have been developed [2,3]. A MSS, generally speaking, is composed of a family of interconnected subsystems that correspond to different modes (subsystems) and switch from one mode to another under the control of a continuous- or discrete-time Markov Process. The mode remains the same between any two consecutive random switches. MSSs, therefore, have been applied in many practical systems, including target tracking systems [4], networked control systems [5], wheeled mobile manipulators [6], and tunnel diode circuits [7].

The duration between any two successive random switches in MSSs, also known as the sojourn time, is a stochastic variable, follows the exponential distribution (ED) in the continuous-time system domain. The transition rates are constant in terms of the memoryless property of the ED. It means that the switching speed between different modes does not depend on the past of the Markov process [8–11]. This feature limits the application of MSSs to some extent and makes it can only be used to model stochastic systems with constant transition rates. A possible way is to adopt a semi-Markov process instead of a Markov process to characterize the random switches between modes. As stated in [12,13], the sojourn time

* Corresponding author.
E-mail address: jpzhou@ahut.edu.cn (J. Zhou).

https://doi.org/10.1016/j.apm.2023.01.045
0307-904X/

in the semi-Markov process is allowed to obey a more general distribution and the corresponding transition rate is time-varying in contrast to the Markov process. Accordingly, semi-Markov switching systems (semi-MSSs) relax the memoryless restriction in the distribution and have a wider application range than MSSs [14]. Hence, it is of considerable theoretical and practical interest to analyze and control semi-MSSs.

A practical semi-MSSs is subject to external disturbances to different degrees. The disturbances may worsen the system performance and even lead to control failure. To reach a satisfactory effect, various control strategies against disturbances, including $\mathscr{H}_\infty$ control [15–17], $\mathscr{L}_2-\mathscr{L}_\infty$ control [18–20], and passive control [21], have been used to semi-MSSs. The extended dissipativity performance index introduced in [22] is comprehensive, covering $\mathscr{H}_\infty$, $\mathscr{L}_2-\mathscr{L}_\infty$, and passivity performance indexes as special cases. For this reason, extended dissipativity control of semi-MSSs has attracted growing attention over recent years. In [23], a non-fragile control approach based on linear matrix inequlities (LMIs) was presented for ensuring the consensus and extended dissipativity of semi-Markov switching multiagent systems. In [24], a state-feedback extended dissipativity control method was proposed for semi-Markov switching neural networks with uncertain transition rates. A class of delayed singular semi-MSSs were considered in [25], where an anti-disturbance extended dissipativity controller design was developed.

With the development of communication technologies, event-triggered control (ETC) has become a spotlight in the control community as it is a perfect candidate for relieving the over-occupation of communication channels [26]. A new measurement will be sent to update the data of the controller only when the change of system states exceeds a certain preset threshold in the trigger condition. By using the ETC, one can achieve a balance between the improvement of resource utilization and expected system performance by setting specific trigger conditions. To date, several meaningful event-triggered mechanisms (ETMs) have been put forward, including the continuous ETM [27], periodic ETM [28], and switched ETM (SETM) [29]. As shown in [29], the time intervals between any two successively triggered moments are not less than a predefined positive constant, therefore avoiding the so-called Zeno phenomenon effectively. In addition, the SETM can significantly reduce the number of triggered events (NTEs) compared to other ETMs. Subsequent research results further confirmed the effectiveness and efficiency such a ETM [30–33]. Summing up the above discussion, this paper focuses on the issue of extended dissipativity stabilization for semi-MSSs based on switched ETC. Our contributions are summarized as follows:

(1) A new SETM, where the threshold function contains a mode-dependent event-triggered matrix and a disturbance term, is introduced to determine the triggered moments. Compared with some existing SETMs, the proposed mode- and disturbance-dependent SETM (MDSETM) can further reduce the NTEs while maintaining control performance.
(2) A criterion for stochastic stability and extended dissipativity of the closed-loop semi-MSSs is established by applying a time- and mode-dependent piecewise-defined Lyapunov functional (LF), the Jensen inequality, and the generalized Dynkin formula.
(3) The issue of extended dissipativity stabilization is addressed via using the established criterion and some equivalent transformations of matrix inequalities. A co-design for the needed feedback-gain and event-triggered matrices is proposed based on a feasible solution of LMIs.

Notations: We use $\mathcal{N}^+$, $\mathbb{R}^l$, and $\mathbb{R}^{l\times m}$ to represent the collection of non-negative integers, l-dimensional Euclidean space, as well as the collection of $l\times m$ real matrices, respectively. $\mathscr{L}_2[0,\infty)$ refers to the space of square-integrable vector functions over $[0,\infty)$. We denote a diagonal matrix by $diag\{\cdot\}$, use symbol $*$ to represent a term in a symmetrical matrix that can be inferred by the symmetric feature, and use $col\{z_1,z_2\}$ to represent a column vector with entries z_1 and z_2. For a square matrix Z, we use $Z>0$ to stand for that Z is symmetric positive definite, $Z\geq 0$ to stand for that Z is semi-positive definite, and $\mathcal{S}(Z)$ to stand for $\mathcal{S}(Z)=Z+Z^T$. Furthermore, we denote by $||\cdot||$ the Euclidean vector norm and use $\mathcal{E}\{\cdot\}$ to denote the mathematical expectation operator.

2. Preliminaries

Consider the following uncertain semi-MSS with disturbances:

$$\begin{aligned}\dot{x}(t)&=\bar{A}(\varsigma(t))x(t)+B(\varsigma(t))u(t)+C(\varsigma(t))\varpi(t),\\ y(t)&=D(\varsigma(t))x(t),\\ x(0)&=0,\quad \varsigma(0)=\varsigma_0,\end{aligned}\tag{1}$$

where where $x(t)\in\mathbb{R}^{n_a}$ is the state of the semi-MSS; $u(t)\in\mathbb{R}^{n_b}$ is the control input; $y(t)\in\mathbb{R}^{n_b}$ is the output; $\varpi(t)\in\mathbb{R}^k$ denotes the external disturbances belong to $\mathscr{L}_2[0,\infty)$; $\bar{A}(\varsigma(t))=A(\varsigma(t))+\Delta A(\varsigma(t))$, $B(\varsigma(t))$, $C(\varsigma(t))$, $D(\varsigma(t))$ are system parameter matrices with proper dimensions; $\Delta A(\varsigma(t))$ represents the system uncertainty; $\{\varsigma(t),t\geq 0\}$ is a semi-Markov process that takes its values in $\bar{N}=\{1,2,\cdots,N\}$, $N\in\mathcal{N}^+$. The transition probabilities of $\{\varsigma(t),t\geq 0\}$ satisfy

$$\Pr\{\varsigma(t+\iota)=j|\varsigma(t)=i\}=\begin{cases}\lambda_{ij}(\iota)\iota+o(\iota), & i\neq j,\\ 1+\lambda_{ii}(\iota)\iota+o(\iota), & i=j,\end{cases}$$

where $\iota>0$ denotes the sojourn time, $o(\iota)$ means the higher-order infinitesimal of ι satisfying $lim_{\iota\to 0}o(\iota)/\iota=0$, and $\lambda_{ij}(\iota)$ is the transition rate from mode i to mode j at t with $\lambda_{ij}(\iota)>0$ $(i\neq j)$ and $\lambda_{ii}(\iota)=-\sum_{j=1,j\neq i}^{N}\lambda_{ij}(\iota)$ [34].

Remark 1. The semi-MSS in (1) consists of a set of continuous-time subsystems and a switching signal obeying the semi-Markov process. Many complex systems in electrical and mechanical engineering, such as the boost converter circuit [35], the DC motor [36,37], and the robotic arm [38], can be modeled as such a system. The semi-Markov process, in which the transition rate depends upon the sojourn time, is more general than the usual Markov process. Therefore, the semi-MSS under consideration possesses a broad application potential.

For semi-MSS in (1), the following three assumptions are made:

Assumption 1. [39] The parameter pair $(\bar{A}(\varsigma(t)),\ B(\varsigma(t)))$ is controllable.

Assumption 2. [40] The disturbances are measurable.

Assumption 3. [41,42] The parameter uncertainty satisfies

$$\Delta A(\varsigma(t)) = E(\varsigma(t))\Delta(t)F(\varsigma(t)), \tag{2}$$

where matrices $E(\varsigma(t))$ and $F(\varsigma(t))$ are known; matrix $\Delta(t)$ is unknown but satisfy $\Delta^T(t)\Delta(t) \le I$.

Remark 2. Controllability, which concerns the ability to provide acceptable dynamic performance through feedback control, is a fundamental property of a control system. The measurability assumption of disturbances, which has been used in many references, will play a significant role in subsequent ETM design. The parameter uncertainty is assumed to have a norm-bounded form, which is more general than the usual interval uncertainty form [43].

The stabilization issue of semi-MSS (1) will be discussed under the frame of a MDSETM-based control. The controller, which is updated at time moments

$$0 = t_0 < t_1 < t_2 < \cdots < t_s < \cdots,\ \lim_{s\to\infty} t_s = \infty,$$

is given as

$$u(t) = B(\varsigma(t))K(\varsigma(t))x(t_s),\ \ t \in [t_s, t_{s+1}),\ \ s = 0, 1, 2, \cdots \tag{3}$$

The event-trigger condition to determine the triggered moments is given as

$$t_{s+1} = \min\{t \ge t_s + d | (x(t) - x(t_s))^T \Lambda(\varsigma(t))(x(t) - x(t_s)) \ge \sigma x^T(t)\Lambda(\varsigma(t))x(t) + \delta\varpi^T(t)\varpi(t)\} \tag{4}$$

with scalars $\sigma \ge 0,\ d > 0,\ \delta \ge 0$, where $\Lambda(\varsigma(t)) \ge 0$ is a mode-dependent event-triggered matrix and d denotes the lowest sampling period. The following is the working principle of the MDSETM: Suppose that the controller receives the measurement at time moment t_s. Then, the sensor will suspend sending measurement for d seconds. When t comes to time moment $t_s + d$, the sensor begins to continuously monitor event-trigger condition (4). If the condition is met, then the sensor will send a new measurement to update controller (3) at trigger moment t_{s+1}. In this way, the time intervals between any two successively triggered moments are not less than d, therefore avoiding the Zeno phenomenon effectively.

Under the proposed MDSETM, the controller in (3) can be recast as

$$u(t) = \begin{cases} B(\varsigma(t))K(\varsigma(t))x(t - \theta(t)),\ \ t \in [t_s, t_s + d), & \text{(5a)} \\ B(\varsigma(t))K(\varsigma(t))[x(t) + e(t)],\ \ t \in [t_s + d, t_{s+1}) & \text{(5b)} \end{cases}$$

with $\theta(t) = t - t_s \le d,\ t \in [t_s,\ t_s + d),\ \ e(t) = x(t_s) - x(t),\ \ t \in [t_s + d, t_{s+1})$. Accordingly, we are able to transform semi-MSS (1) into the following switched system:

$$\dot{x}(t) = \begin{cases} \bar{A}(\varsigma(t))x(t) + C(\varsigma(t))\varpi(t) + B(\varsigma(t))K(\varsigma(t))x(t - \theta(t)),\ \ t \in [t_s, t_s + d), & \text{(6a)} \\ \bar{A}(\varsigma(t))x(t) + C(\varsigma(t))\varpi(t) + B(\varsigma(t))K(\varsigma(t))[x(t) + e(t)],\ \ t \in [t_s + d, t_{s+1}). & \text{(6b)} \end{cases}$$

Letting $\varsigma(t) = i \in \bar{N}$, the $A_i,\ B_i,\ C_i,\ D_i,\ \Delta A_i,\ E_i,\ F_i,\ \bar{A}_i,\ K_i,\ \Lambda_i$ are used to replace the matrices in system (1), which is beneficial to simplicity of notation.

Remark 3. Under the proposed MDSETM, the controller allows periodic sampling for $t \in [t_s, t_s + d)$ and continuous event triggering for $t \in [t_s + d, t_{s+1})$, resulting in a switched closed-loop system (SCLS). When $\Lambda(\varsigma(t)) = \Lambda$, the event-triggered matrix is mode-independent, and the MDSETM will reduces to the SETM given in [44]; when further restricting $\delta = 0$, the threshold function is independent of disturbances, and the MDSETM will reduces to the SETM given in [29]. Compared to the periodic sampling mechanism (PSM) in [45] and SETMs in [29,44], the introduction of a mode-dependent event-triggered matrix and disturbance term into the threshold function contributes to further reducing the NTEs while maintaining control performance, which will be demonstrated in Section 4.

We recall the following two concepts and two lemma:

Definition 1. [46] Semi-MSS (1) with all modes is said to be stochastically stable if, when $\varpi(t) = 0$, there exist a positive scalar $M_\diamond$ such that

$$\mathcal{E}\left(\int_0^\infty ||x(\mu)||^2 d\mu\right) \le M_\diamond. \tag{7}$$

Definition 2. [22] For given real matrices Υ_i $(i = 1, \cdots, 4)$ satisfying $\Upsilon_1 \le 0$, Υ_2, $\Upsilon_3 > 0$, $\Upsilon_4 \ge 0$ and $(||\Upsilon_1|| + ||\Upsilon_2||)||\Upsilon_4|| = 0$, suppose, under condition $x(0) = 0$,

$$\sup_{t\ge 0}\left\{\mathcal{E}\left(x^T(t)\Upsilon_4 x(t)\right)\right\} \le \mathcal{E}\left(\int_0^t J(\mu)pd\mu\right) \tag{8}$$

holds for any $t \ge 0$, where

$$J(t) = x^T(t)\Upsilon_1 x(t) + 2x^T(t)\Upsilon_2\varpi(t) + \varpi^T(t)\Upsilon_3\varpi(t).$$

Then, semi-MSS (6) is said to be extended dissipative.

Lemma 1. *[47, 48] (Jensen's inequality) For any $l \times l$ dimensions matrix $W > 0$, scalars a_1 and a_2 with $a_2 > a_1$, and vector function $\delta : [a_1, a_2] \to \mathbb{R}^l$,*

$$\frac{1}{(a_2 - a_1)}\int_{a_1}^{a_2}\delta^T(\mu)d\mu W\int_{a_1}^{a_2}\delta(\mu)d\mu \le \int_{a_1}^{a_2}\delta^T(\mu)W\delta(\mu)d\mu$$

holds.

Lemma 2. *[49] For proper dimensions matrices L_1 $(L_1^T = L_1)$, L_2, L_3, and $\Delta(t)$ $(\Delta^T(t)\Delta(t) \le I)$,*

$$L_1 + \mathcal{S}\left(L_3\Delta(t)L_2\right) < 0$$

holds if and only if there is a constant $\epsilon > 0$ such that

$$L_1 + \epsilon^{-1}L_3L_3^T + \epsilon L_2^TL_2 < 0.$$

Remark 4. The extended dissipativity, which has been widely studied for a variety of control systems; see, e.g., [50–52], is quite comprehensive. In fact, the extended dissipativity condition in (8) can be transformed into the $\mathscr{H}_\infty$ performance condition by setting $\Upsilon_1 = -I$, $\Upsilon_2 = 0$, $\Upsilon_3 = \gamma^2 I$, $\Upsilon_4 = 0$ [15–17], $\mathscr{L}_2 - \mathscr{L}_\infty$ performance condition by setting $\Upsilon_1 = 0$, $\Upsilon_2 = 0$, $\Upsilon_3 = \gamma^2 I$, $\Upsilon_4 = I$ [18–20], the passivity performance condition by setting $\Upsilon_1 = 0$, $\Upsilon_2 = I$, $\Upsilon_3 = \gamma I$, $\Upsilon_4 = 0$ [21], as well as $(\mathscr{Q}, \mathscr{S}, \mathscr{R})$ -dissipativity performance condition by setting $\Delta_1 = Q$, $\Delta_2 = S$, $\Delta_3 = R - \gamma I$, $\Delta_4 = 0$ [53].

In this paper, we are intended to achieve the extended dissipativity stabilization of semi-MSSs via utilizing the proposed the MDSETM. To be specific, we would like to determine the feedback-gain matrix in (3) and event-triggered matrices in (4) for ensuring that uncertain semi-MSS in (1) is not only stochastically stable but also extended dissipative.

3. Main results

First, we give a result for the need performance analysis of semi-MSS (6).

Theorem 1. *For given real matrices $\Upsilon_1 \le 0$, Υ_2, $\Upsilon_3 > 0$, and $\Upsilon_4 \ge 0$ satisfying $(||\Upsilon_1|| + ||\Upsilon_2||) \cdot ||\Upsilon_4|| = 0$, and scalars ε_1, ε_2, $\gamma > 0$, $\delta \ge 0$, $d > 0$, $\alpha > 0$, $\sigma \ge 0$, suppose that, for any $i \in \bar{N}$, there exist matrices $P_i > 0$, $U > 0$, $\bar{Q} = \begin{bmatrix} Q_1 & Q_2 \\ * & Q_3 \end{bmatrix} > 0$, Y, H_m $(m = 1, 2, 3, 4, 5)$, G_n $(n = 1, 2, 3, 4)$ and matrix $\Lambda_i \ge 0$ such that*

$$\Psi(i) = \begin{bmatrix} \Psi_{11}(i) & \Psi_{12}(i) & \Psi_{13}(i) & \Psi_{14} & \Psi_{15}(i) & \Psi_{16} \\ * & \Psi_{22} & \Psi_{23}(i) & 0 & \Psi_{25}(i) & \Psi_{26} \\ * & * & \Psi_{33}(i) & \Psi_{34} & \Psi_{35}(i) & \Psi_{36} \\ * & * & * & \Psi_{44} & 0 & \Psi_{46} \\ * & * & * & * & \Psi_{55} & 0 \\ * & * & * & * & * & \Psi_{66} \end{bmatrix} < 0, \tag{9}$$

$$\Theta(i) = \begin{bmatrix} \Theta_{11}(i) & \Theta_{12}(i) & \Theta_{13}(i) & \Theta_{14} & \Theta_{15}(i) \\ * & \Theta_{22} & \Theta_{23}(i) & \Theta_{24} & \Theta_{25}(i) \\ * & * & \Theta_{33}(i) & \Theta_{34} & \Theta_{35}(i) \\ * & * & * & \Theta_{44} & 0 \\ * & * & * & * & \Theta_{55} \end{bmatrix} < 0, \tag{10}$$

$$\Phi(i) = \begin{bmatrix} \Phi_{11}(i) & \Phi_{12}(i) & \Phi_{13}(i) & \Phi_{14}(i) \\ * & \Phi_{22} & \Phi_{23}(i) & \Phi_{24}(i) \\ * & * & \Phi_{33}(i) & 0 \\ * & * & * & \Phi_{44} \end{bmatrix} < 0, \tag{11}$$

$$\Xi(i)=\begin{bmatrix} P_i+d\mathcal{S}(\frac{H_1}{2})-\Upsilon_4 & -dH_1+dH_2 & dH_3 \\ * & -d\mathcal{S}(H_2-\frac{H_1}{2}) & dH_4 \\ * & * & d\mathcal{S}(\frac{H_5}{2}) \end{bmatrix}>0, \tag{12}$$

$$P_i-\Upsilon_4>0 \tag{13}$$

hold, where

$$\begin{aligned}
\Psi_{11}(i)&=\textstyle\sum_{j=1}^{N}\lambda_{ij}^{*}P_j+2\alpha P_i+\mathcal{S}\big(-\frac{H_1}{2}+G_1+Y\bar{A}_i\big)-\mathrm{Y}_1,\\
\Psi_{12}(i)&=P_i+G_2-Y+\varepsilon_1\bar{A}_i^{T}Y^{T},\\
\Psi_{13}(i)&=H_1-H_2+G_3-G_1^{T}+YB_iK_i+\varepsilon_2\bar{A}_i^{T}Y^{T},\\
\Psi_{14}&=-H_3+G_4,\ \Psi_{15}(i)=YC_i-\mathrm{Y}_2,\\
\Psi_{16}&=\sqrt{d}G_1^{T},\ \Psi_{22}=-\mathcal{S}(\varepsilon_1Y),\\
\Psi_{23}(i)&=-G_2^{T}-\varepsilon_2Y^{T}+\varepsilon_1YB_iK_i,\\
\Psi_{25}(i)&=\varepsilon_1YC_i,\ \Psi_{26}=\sqrt{d}G_2^{T},\\
\Psi_{33}(i)&=\mathcal{S}\big(H_2-\tfrac{H_1}{2}-G_3+\varepsilon_2YB_iK_i\big)-de^{-2\alpha d}Q_3,\\
\Psi_{34}&=-H_4-e^{-2\alpha d}Q_2^{T}-G_4,\ \Psi_{35}(i)=\varepsilon_2YC_i,\ \Psi_{36}=\sqrt{d}G_3^{T},\\
\Psi_{44}&=-\mathcal{S}\big(\tfrac{H_5}{2}\big)-\tfrac{e^{-2\alpha d}}{d}Q_1,\ \Psi_{46}=\sqrt{d}G_4^{T},\\
\Psi_{55}&=-\mathrm{Y}_3,\ \Psi_{66}=-e^{-2\alpha d}U,\\
\Phi_{11}(i)&=\textstyle\sum_{v=1,j}^{N}\lambda_{ij}^{*}P_j+2\alpha P_i+\sigma\Lambda_i+\mathcal{S}\big(Y\bar{A}_i+YB_iK\big)-\mathrm{Y}_1,\\
\Phi_{12}(i)&=P_i-Y+\varepsilon_1\bar{A}_i^{T}Y^{T}+(\varepsilon_1YB_iK_i)^{T},\\
\Phi_{13}(i)&=YB_iK_i,\ \Phi_{14}(i)=YC_i-\mathrm{Y}_2,\\
\Phi_{22}&=\mathcal{S}(-\varepsilon_1Y),\ \Phi_{23}(i)=\varepsilon_1YB_iK_i,\ \Phi_{24}(i)=\varepsilon_1YC_i,\\
\Phi_{33}(i)&=-\Lambda_i,\ \Phi_{44}=\delta I-\mathrm{Y}_3,\\
\Theta_{11}(i)&=\Psi_{11}(i)+\alpha d\mathcal{S}(H_1)+d\mathcal{S}(H_3)+dQ_1-\mathrm{Y}_1,\\
\Theta_{12}(i)&=\Psi_{12}(i)+d\tfrac{\mathcal{S}(H_1)}{2},\\
\Theta_{13}(i)&=\Psi_{13}(i)+2\alpha d(H_2-H_1)+dH_4^{T}+dQ_2,\\
\Theta_{14}&=\Psi_{14}+2\alpha dH_3+d\tfrac{\mathcal{S}(H_5)}{2},\ \Theta_{15}(i)=YC_i-\mathrm{Y}_2\\
\Theta_{22}&=\Psi_{22}+dU,\ \Theta_{23}(i)=\Psi_{23}(i)+d(H_2-H_1),\\
\Theta_{24}&=dH_3,\ \Theta_{25}(i)=\varepsilon_1YC_i,\\
\Theta_{33}(i)&=\mathcal{S}\big(H_2-\tfrac{H_1}{2}-G_3+\varepsilon_2YB_iK_i\big)+2\alpha d\mathcal{S}\big(-H_2+\tfrac{H_1}{2}\big)+dQ_3,\\
\Theta_{34}&=\Psi_{34}+2\alpha dH_4,\ \Theta_{35}(i)=\varepsilon_2YC_i\\
\Theta_{44}&=\Psi_{44}+\alpha d\mathcal{S}(H_5),\ \Theta_{55}=-\mathrm{Y}_3,\ \lambda_{ij}^{*}=\mathcal{E}\big\{\lambda_{ij}(\iota)\big\}.
\end{aligned}$$

Then, semi-MSS (6) is stochastic stable and extended dissipative.

Proof. Consider time- and mode-dependent piecewise-defined LF:

$$V(t,\varsigma(t))=\begin{cases}V_\alpha(t,\varsigma(t)),\ t\in[t_s,t_s+d),\\ V_\beta(t,\varsigma(t)),\ t\in[t_s+d,t_{s+1}),\end{cases}$$

where $V_\alpha(t,\varsigma(t))=\sum_{m=1}^{4}V_m(t,\varsigma(t))$, $V_\beta(t,\varsigma(t))=V_1(t,\varsigma(t))$ with

$$\begin{aligned}
V_1(t,\varsigma(t))&=e^{2\alpha t}x^{T}(t)P_{\varsigma(t)}x(t),\\
V_2(t,\varsigma(t))&=\theta_d(t)\int_{t-\theta(t)}^{t}e^{2\alpha\mu}\dot{x}^{T}(\mu)U\dot{x}(\mu)d\mu,\\
V_3(t,\varsigma(t))&=\theta_d(t)\int_{t-\theta(t)}^{t}e^{2\alpha\mu}\eta_1^{T}(\mu)\bar{Q}\eta_1(\mu)d\mu,\\
V_4(t,\varsigma(t))&=\theta_d(t)e^{2\alpha t}\eta_2^{T}(t)\mathcal{F}\eta_2(t),
\end{aligned}$$

and

$$\theta_d(t) = d - \theta(t),\ \ \eta_1(\mu) = col\{x(\mu), x(\mu-\theta(\mu))\},$$

$$\eta_2(t) = col\left\{x(t), x(t-\theta(t)), \int_{t-\theta(t)}^{t} x(\mu)d\mu\right\},$$

$$\mathcal{F} = \begin{bmatrix} \mathcal{S}(\frac{H_1}{2}) & -H_1+H_2 & H_3 \\ * & \mathcal{S}(-H_2+\frac{H_1}{2}) & H_4 \\ * & * & \mathcal{S}(\frac{H_5}{2}) \end{bmatrix}.$$

Note that

$$\begin{aligned} &V_1(t,\varsigma(t)) + V_4(t,\varsigma(t)) \\ &= e^{2\alpha t}\eta_2^T(t)\begin{bmatrix} P_{\varsigma(t)} + \theta_d(t)\mathcal{S}\left(\frac{H_1}{2}\right) & \theta_d(t)(-H_1+H_2) & \theta_d(t)H_3 \\ * & \theta_d(t)\mathcal{S}\left(-H_2+\frac{H_1}{2}\right) & \theta_d(t)H_4 \\ * & * & \theta_d(t)\mathcal{S}\left(\frac{H_5}{2}\right) \end{bmatrix}\eta_2(t) \\ &= e^{2\alpha t\frac{\theta(t)}{d}}\eta_2^T(t)\left(\begin{bmatrix} P_{\varsigma(t)} - \Upsilon_4 & 0 & 0 \\ 0 & 0 & 0 \\ 0 & 0 & 0 \end{bmatrix} + \begin{bmatrix} \Upsilon_4 & 0 & 0 \\ 0 & 0 & 0 \\ 0 & 0 & 0 \end{bmatrix}\right)\eta_2(t) \\ &\quad + e^{2\alpha t\frac{\theta_d(t)}{d}}\eta_2^T(t)\left(\Xi(i) + \begin{bmatrix} \Upsilon_4 & 0 & 0 \\ 0 & 0 & 0 \\ 0 & 0 & 0 \end{bmatrix}\right)\eta_2(t), \end{aligned}$$

which, together with $P_i > 0$ $(i \in \tilde{N})$, $U > 0$, $\tilde{Q} > 0$, $\Upsilon_4 \geq 0$, (12), and (13), gives

$$V(t,\varsigma(t)) \geq V_1(t,\varsigma(t)) + V_4(t,\varsigma(t)) \geq e^{2\alpha t}\eta_2^T(t)\begin{bmatrix} \Upsilon_4 & 0 & 0 \\ 0 & 0 & 0 \\ 0 & 0 & 0 \end{bmatrix}\eta_2(t) \geq x^T(t)\Upsilon_4 x(t). \tag{14}$$

It results from (14) that the constructed functional $V(t)$ is positive definite.

Consider the following two cases in light of two different time intervals:

Case I $t \in [t_s, t_s + d)$

In this case, we have $V(t,\varsigma(t)) = V_\alpha(t,\varsigma(t))$. Denote by $\mathcal{L}$ the infinitesimal operator. Then, for $\varsigma(t) = i$, we can achieve that

$$\begin{aligned} \mathcal{L}V(t,\varsigma(t)=i) &= \lim_{\xi\to 0}\frac{\mathbb{E}[V(x(t+\xi),\varsigma(t+\xi))|x(t),\varsigma(t)] - V(x(t),\varsigma(t))}{\xi} \\ &= \lim_{\xi\to 0}\frac{1}{\xi}\Bigg[\sum_{j=1,j\neq i}^{N}\Pr(\varsigma(t+\xi)=j|\varsigma(t)=i)e^{2\alpha(t+\xi)}x^T(t+\xi)P_j x(t+\xi) \\ &\quad + \Pr(\varsigma(t+\xi)=i|\varsigma(t)=i)e^{2\alpha(t+\xi)}x^T(t+\xi)P_i x(t+\xi) - e^{2\alpha t}x^T(t)P_i x(t)\Bigg] \\ &= \lim_{\xi\to 0}\frac{1}{\xi}\Bigg[\sum_{j=1,j\neq i}^{N}\frac{\Pr(\varsigma(t+\xi)=j,\varsigma(t)=i)}{\Pr\{\varsigma(t)=i\}}e^{2\alpha(t+\xi)}x^T(t+\xi)P_j x(t+\xi) \\ &\quad + \frac{\Pr(\varsigma(t+\xi)=i,\varsigma(t)=i)}{\Pr\{\varsigma(t)=i\}}e^{2\alpha(t+\xi)}x^T(t+\xi)P_i x(t+\xi) - e^{2\alpha t}x^T(t)P_i x(t)\Bigg] \\ &= \lim_{\xi\to 0}\frac{1}{\xi}\Bigg[\sum_{j=1,j\neq i}^{N}(\lambda_{ij}(\iota)\iota + o(\iota))e^{2\alpha(t+\xi)}x^T(t+\xi)P_j x(t+\xi) \\ &\quad + (1+\lambda_{ii}(\iota)\iota + o(\iota))e^{2\alpha(t+\xi)}x^T(t+\xi)P_i x(t+\xi) - e^{2\alpha t}x^T(t)P_i x(t)\Bigg]. \end{aligned}$$

It suggests that

$$\mathcal{L}V_1(t,\varsigma(t)=i) = \sum_{j=1}^{N}\lambda_{ij}(\iota)e^{2\alpha t}x^T(t)P_jx(t) + 2\alpha e^{2\alpha t}x^T(t)P_ix(t) + 2e^{2\alpha t}x^T(t)P_i\dot{x}(t), \tag{15}$$

$$\begin{aligned}\mathcal{L}V_2(t,\varsigma(t)=i) &= \theta_d(t)e^{2\alpha t}\dot{x}^T(t)U\dot{x}(t) - \int_{t-\theta(t)}^{t} e^{2\alpha\mu}\dot{x}^T(\mu)U\dot{x}(\mu)d\mu\\ &\le \theta_d(t)e^{2\alpha t}\dot{x}^T(t)U\dot{x}(t) - \int_{t-\theta(t)}^{t} e^{2\alpha t_s}\dot{x}^T(\mu)U\dot{x}(\mu)d\mu\\ &\le \theta_d(t)e^{2\alpha t}\dot{x}^T(t)U\dot{x}(t) - e^{2\alpha t}\int_{t-\theta(t)}^{t} e^{-2\alpha d}\dot{x}^T(\mu)U\dot{x}(\mu)d\mu,\end{aligned} \tag{16}$$

$$\begin{aligned}\mathcal{L}V_3(t,\varsigma(t)=i) &= -\int_{t-\theta(t)}^{t} e^{2\alpha\mu}\eta_1^T(\mu)\overline{Q}\eta_1(\mu)d\mu + \theta_d(t)e^{2\alpha t}\eta_1^T(t)\overline{Q}\eta_1(t)\\ &\le -\int_{t-\theta(t)}^{t} e^{2\alpha(t-\theta(t))}\eta_1^T(\mu)\overline{Q}\eta_1(\mu)d\mu + \theta_d(t)e^{2\alpha t}\eta_1^T(t)\overline{Q}\eta_1(t)\\ &\le -e^{2\alpha t}\int_{t-\theta(t)}^{t} e^{-2\alpha d}\eta_1^T(\mu)\overline{Q}\eta_1(\mu)d\mu + \theta_d(t)e^{2\alpha t}\eta_1^T(t)\overline{Q}\eta_1(t)\\ &= -e^{2\alpha t}\int_{t-\theta(t)}^{t} e^{-2\alpha d}x^T(\mu)Q_1x(\mu)d\mu - 2e^{2\alpha t}x^T(t-\theta(t))e^{-2\alpha d}Q_2^T\int_{t-\theta(t)}^{t}x(\mu)d\mu\\ &\quad -\theta(t)e^{2\alpha t}x^T(t-\theta(t))e^{-2\alpha d}Q_3x(t-\theta(t)) + \theta_d(t)e^{2\alpha t}\eta_1^T(t)\overline{Q}\eta_1(t),\end{aligned} \tag{17}$$

$$\begin{aligned}\mathcal{L}V_4(t,\varsigma(t)=i) &= -e^{2\alpha t}\eta_2^T(t)\mathcal{F}\eta_2(t) + 2\alpha\theta_d(t)e^{2\alpha t}\eta_2^T(t)\mathcal{F}\eta_2(t) + 2\theta_d(t)e^{2\alpha t}\eta_2^T(t)\mathcal{F}\eta_2(t)\\ &\le -e^{2\alpha t}\eta_2^T(t)\mathcal{F}\eta_2(t) + 2\alpha\theta_d(t)e^{2\alpha t}\eta_2^T(t)\mathcal{F}\eta_2(t)\\ &\quad +2\theta_d(t)e^{2\alpha t}x^T(t)\frac{H_1+H_1^T}{2}\dot{x}(t) + 2\theta_d(t)e^{2\alpha t}x^T(t-\theta(t))(-H_1+H_2)^T\dot{x}(t)\\ &\quad +2\theta_d(t)e^{2\alpha t}\int_{t-\theta(t)}^{t}x^T(\mu)d\mu{H_3}^T\dot{x}(t) + 2\theta_d(t)e^{2\alpha t}x^T(t)H_3x(t)\\ &\quad +2\theta_d(t)e^{2\alpha t}x^T(t-\theta(t))H_4x(t) + 2\theta_d(t)e^{2\alpha t}\int_{t-\theta(t)}^{t}x^T(\mu)d\mu\frac{H_5+H_5^T}{2}x(t).\end{aligned} \tag{18}$$

Using Lemma 1, we have

$$-\int_{t-\theta(t)}^{t} e^{-2\alpha d}x^T(\mu)Q_1x(\mu)d\mu \le -\int_{t-\theta(t)}^{t}x^T(\mu)d\mu\frac{e^{-2\alpha d}}{d}Q_1\int_{t-\theta(t)}^{t}x(\mu)d\mu. \tag{19}$$

Applying (19) to (17), we can obtain

$$\begin{aligned}&\mathcal{L}V_3(t,\varsigma(t)=i)\\ &\le -e^{2\alpha t}\int_{t-\theta(t)}^{t}x^T(\mu)d\mu\frac{e^{-2\alpha d}}{d}Q_1\int_{t-\theta(t)}^{t}x(\mu)d\mu - 2e^{2\alpha t}x^T(t-\theta(t))e^{-2\alpha d}Q_2^T\int_{t-\theta(t)}^{t}x(\mu)d\mu\\ &\quad -(t-t_s)e^{2\alpha t}x^T(t-\theta(t))e^{-2\alpha d}Q_3x(t-\theta(t)) + (t_{s+1}-t)e^{2\alpha t}\eta_1^T(t)\bar{Q}\eta_1(t).\end{aligned} \tag{20}$$

For matrix G with proper dimension, based on Schur's complement, we have

$$\begin{bmatrix} G^Te^{2\alpha d}U^{-1}G & G^T\\ * & e^{-2\alpha d}U\end{bmatrix} \ge 0,$$

which implies

$$\int_{t-\theta(t)}^{t}\begin{bmatrix}\phi(t)\\ \dot{x}(\mu)\end{bmatrix}^T\begin{bmatrix} G^Te^{2\alpha d}U^{-1}G & G^T\\ * & e^{-2\alpha d}U\end{bmatrix}\begin{bmatrix}\phi(t)\\ \dot{x}(\mu)\end{bmatrix}d\mu \ge 0, \tag{21}$$

where

$$\phi(t) = \mathrm{col}\{x(t),\dot{x}(t),x(t-\theta(t)),\int_{t-\theta(t)}^{t}x(\mu)d\mu\}.$$

From (21) we have

$$-\int_{t-\theta(t)}^{t} e^{-2\alpha d}\dot{x}^T(\mu)U\dot{x}(\mu)d\mu \le \theta(t)\phi^T(t)G^Te^{2\alpha d}U^{-1}G\phi(t) + 2\phi^T(t)G^Tx(t) - 2\phi^T(t)G^Tx(t-\theta(t)). \tag{22}$$

Combining (22) with (18), we obtain

$$\mathcal{L}V_4(t,\varsigma(t)=i) = e^{2\alpha t}\theta(t)\phi^T(t)G^T e^{2\alpha d}U^{-1}G\phi(t) + 2e^{2\alpha t}\phi^T(t)G^T x(t) - 2e^{2\alpha t}\phi^T(t)G^T x(t-\theta(t)) + (t_{s+1}-t)e^{2\alpha t}\dot{x}^T(t)U\dot{x}(t). \tag{23}$$

For any scalars $\varepsilon_1,\ \varepsilon_2$ and matrix Y with appropriate dimension, we have from (6a) that

$$0 = 2e^{2\alpha t}\left[x^T(t)+\varepsilon_1\dot{x}^T(t)+\varepsilon_2 x^T(t-\theta(t))\right]Y\left[-\dot{x}(t)+\bar{A}_i x(t)+C_i\varpi(t)+B_iK_i x(t-\theta(t))\right]. \tag{24}$$

Then, we obtain from (15), (16), (20), (23), and (24) that for $t\in[t_s,t_s+d)$,

$$\mathcal{E}\{\mathcal{L}V_\alpha(t,\varsigma(t)=i)-J(t)\} \le \mathcal{E}\{e^{2\alpha t}\phi^T(t)\Psi_2(i)\phi(t)\}.$$

where

$$\Psi_2(i) = \left[\tfrac{\theta_d(t)}{d}\Theta(i) + \tfrac{\theta(t)}{d}\widetilde{\Psi}(i)\right],$$

$$\widetilde{\Psi}(i) = \begin{bmatrix} \Psi_{11}(i) & \Psi_{12}(i) & \Psi_{13}(i) & \Psi_{14} & \Psi_{15}(i) \\ * & \Psi_{22} & \Psi_{23}(i) & 0 & \Psi_{25}(i) \\ * & * & \Psi_{33}(i) & \Psi_{34} & \Psi_{35}(i) \\ * & * & * & \Psi_{44} & 0 \\ * & * & * & * & \Psi_{55} \end{bmatrix} + d\begin{bmatrix} G_1^T \\ G_2^T \\ G_3^T \\ G_4^T \\ 0 \end{bmatrix} e^{2\alpha d}U^{-1}\begin{bmatrix} G_1^T \\ G_2^T \\ G_3^T \\ G_4^T \\ 0 \end{bmatrix}^T.$$

From (9), (10), and Schur's complement, there is a positive constant M_1 such that

$$\mathcal{E}\{\mathcal{L}V_\alpha(t,\varsigma(t)=i)-J(t)\} \le -M_1||x(t)||^2,\ t\in[t_s,t_s+d).$$

Case II $t\in[t_s+d,t_{s+1})$.

In this situation, we have $V(t,\varsigma(t)) = V_\beta(t,\varsigma(t))$. Event-trigger condition (4) implies

$$0 \le -e^T(t)\Lambda_i e(t) + \sigma x^T(t)\Lambda_i x(t) + \delta\varpi^T(t)\varpi(t). \tag{25}$$

By (6b), we have

$$0 = 2e^{2\alpha t}\left[x^T(t)Y+\dot{x}^T(t)\varepsilon_1 Y\right]\left[-\dot{x}(t)+\bar{A}_i x(t)+C_i\varpi(t)+B_iK_i(x(t)+e(t))\right]. \tag{26}$$

Using (11), (25), (26), and following a similar proof process of Case *I*, we can show that there is a positive constant M_2 such that

$$\mathcal{E}\{\mathcal{L}V_\beta(t,\varsigma(t)=i)-J(t)\} \le \mathcal{E}\{e^{2\alpha t}\phi_1^T(t)\Phi(i)\phi_1(t)\} \le -M_2||x(t)||^2,\ t\in[t_s+d,t_{s+1}),$$

where $\phi_1(t) = \mathrm{col}\{x(t),\ \dot{x}(t),\ e(t)\}$.

Combining these two cases, we have

$$\mathcal{E}\{\mathcal{L}V(t,\varsigma(t)=i)-J(t)\} \le -M_0||x(t)||^2,\ t\in[t_s,t_{s+1}), \tag{27}$$

where $M_0 = \max\{M_1, M_2\}$. Applying the generalized Dynkin formula [46], from (27) we can write

$$\begin{aligned} &\mathcal{E}\left\{V(x(t),\varsigma(t)=i) - V(x(0),\varsigma(0)) - \int_0^t J(\mu)d\mu\right\} \\ &= \mathcal{E}\left\{V(x(t),\varsigma(t)=i) - V(x(t_s),\varsigma(t_s)) - \int_{t_s}^t J(\mu)d\mu\right\} \\ &\quad + \cdots + V(x(t_1),\varsigma(t_1)) - V(x(0),\varsigma(0)) - \int_0^{t_1} J(\mu)d\mu\Big\} \\ &\le \mathcal{E}\left\{\int_{t_s}^t \{\mathcal{L}V(\mu)-J(\mu)\}d\mu\right\} + \cdots + \mathcal{E}\left\{\int_0^{t_1}\{\mathcal{L}V(\mu)-J(\mu)\}d\mu\right\} \\ &\le -\mathcal{E}\left\{M_0\int_0^t \|x(t)\|^2 d\mu\right\}, \end{aligned} \tag{28}$$

When $\varpi(t)=0$, we have from $\Upsilon_1\le 0$, $V(x(t),\varsigma(t))\ge 0$, and (28) that

$$\begin{aligned} \mathcal{E}\left\{\int_0^t ||x(t)||^2 d\mu\right\} &\le -\frac{1}{M_0}\mathcal{E}\left\{V(x(t),\varsigma(t)=i) - V(x(0),\varsigma(0)) - \int_0^t J(\mu)d\mu\right\} \\ &\le \frac{1}{M_0}\mathcal{E}\{V(x(0),\varsigma(0))\}. \end{aligned}$$

Considering the arbitrariness of t, we have (7) by choosing $M_\circ = \mathcal{E}\{V(x(0), \varsigma(0))\}/M_0$, which means that semi-MSS (6) is stochastic stable.

In what follows, we proceed with the deduction of extended dissipativity. In the case when $x(0) = 0$, from (28) we have

$$\mathcal{E}\left\{\int_0^t J(\mu)d\mu\right\} \geq \mathcal{E}\{V(x(t), \varsigma(t) = i) - V(x(0), \varsigma(0)) \geq \mathcal{E}\{V(x(t), \varsigma(t) = i)\right\}. \tag{29}$$

Using (14) and (29), we have

$$\mathcal{E}\left\{\int_0^t J(\mu)d\mu\right\} \geq \mathcal{E}\{x^T(t)\Upsilon_4 x(t)\right\},$$

which, in conjunction with the arbitrariness of t, leads to (8). Based on Definition 2, semi-MSS (6) is extended dissipative, and the proof is completed. □

Remark 5. Note that, under the effect of the the MDSETM (4), semi-MSS (6) is a switched system in terms of time and parameter. For such a mode-dependent and time-dependent switched system, how to establish an appropriate LF to achieve the control objective for the system is an intricate problem. Motivated by [29,54], a mode-dependent and time-dependent piecewise LF $V(t, \varsigma(t))$ is established. The LF $V(t, \varsigma(t))$ consists of $V_\alpha(t)$ and $V_\beta(t)$ upon difference time intervals. When $t \in [t_s, t_s + d)$, the LF $V_\alpha(t)$ will be employed, while when $t \in [t_s + d, t_{s+1})$, the LF $V_\beta(t)$ will be adopted. In addition, the continuity of the LF $V(t, \varsigma(t))$ at t_s and $t_s + d$ is vital for the stability analysis of semi-MSS. For time moment t_s, $V_2(t_s) = V_3(t_s) = V_4(t_s) = 0$ because of $x(t) = x(t - \theta(t))$, and for time moment $t_s + d$, $\lim_{t\to t_s^- + d} V_2(t) = 0$, $\lim_{t\to t_s^- + d} V_3(t) = 0$ and $\lim_{t\to t_s^- + d} V_4(t) = 0$ due to $\lim_{t\to t_s^- + d}(d - \theta(t)) = 0$. In summary, $V_\alpha(t) = V_\beta(t)$ at moments t_s and $t_s + d$, which indicates $V(t, \varsigma(t))$ is continuous.

Now, we address the extended dissipativity stabilization issue. We can prove the following result:

Theorem 2. *For given real matrices $\Upsilon_1 \leq 0$, Υ_2, $\Upsilon_3 > 0$, $\Upsilon_4 \geq 0$ satisfying $(||\Upsilon_1|| + ||\Upsilon_2||) \cdot ||\Upsilon_4|| = 0$, and scalars ε_1, ε_2, $\gamma > 0$, $\delta \geq 0$, $d > 0$, $\alpha > 0$, $\sigma \geq 0$, suppose that, for any $i \in \bar{N}$, there exist a scalar $\rho > 0$ and matrices $\bar{P}_i > 0$, $\bar{U} > 0$, $\bar{Q} = \begin{bmatrix} \bar{Q}_1 & \bar{Q}_2 \\ * & \bar{Q}_3 \end{bmatrix} > 0$, $\bar{Y}$, $\bar{H}_m$ $(m = 1, 2, 3, 4, 5)$, $\bar{G}_n$ $(n = 1, 2, 3, 4)$, $\bar{K}_i$ and $\bar{\Lambda}_i \geq 0$ such that*

$$\overline{\Psi}(i) = \begin{cases} \overline{\Psi}(i) < 0, \ \Upsilon_1 = 0, \\ \begin{bmatrix} \overline{\Psi}(i) & \tilde{Y}_1 \\ * & \Upsilon_1^{-1} \end{bmatrix} < 0, \ \Upsilon_1 < 0, \end{cases} \tag{30}$$

$$\overline{\Theta}(i) = \begin{cases} \overline{\Theta}(i) < 0, \Upsilon_1 = 0, \\ \begin{bmatrix} \overline{\Theta}(i) & \tilde{Y}_2 \\ * & \Upsilon_1^{-1} \end{bmatrix} < 0, \Upsilon_1 < 0, \end{cases} \tag{31}$$

$$\overline{\Phi}(i) = \begin{cases} \overline{\Phi}(i) < 0, \ \Upsilon_1 = 0, \\ \begin{bmatrix} \overline{\Phi}(i) & \tilde{Y}_3 \\ *\Upsilon_1^{-1} & \end{bmatrix} < 0, \ \Upsilon_1 < 0, \end{cases} \tag{32}$$

$$\overline{\Xi}(i) = \begin{cases} \overline{\Xi}(i) > 0, \ \Upsilon_4 = 0, \\ \begin{bmatrix} \overline{\Xi}(i) & \tilde{Y}_4 \\ *\Upsilon_4^{-1} & \end{bmatrix} > 0, \ \Upsilon_4 > 0, \end{cases} \tag{33}$$

$$\overline{P}_i = \begin{cases} \overline{P}_i > 0, \ \Upsilon_4 = 0, \\ \begin{bmatrix} \overline{P}_i & \overline{Y} \\ *\Upsilon_4^{-1} & \end{bmatrix} > 0, \ \Upsilon_4 > 0, \end{cases} \tag{34}$$

hold, where

$$\overline{\Psi}(i)=\begin{bmatrix}\overline{\Psi}_{11}(i) & \overline{\Psi}_{12}(i) & \Psi_{13}(i) & \overline{\Psi}_{14} & \overline{\Psi}_{15}(i) & \overline{\Psi}_{16} & E_i & \overline{Y}F_i^T\\ & \overline{\Psi}_{22} & \overline{\Psi}_{23}(i) & 0 & \overline{\Psi}_{25}(i) & \overline{\Psi}_{26} & \varepsilon_1E_i & 0\\ & * & \overline{\Psi}_{33}(i) & \overline{\Psi}_{34} & \overline{\Psi}_{35}(i) & \overline{\Psi}_{36} & \varepsilon_2E_i & 0\\ & * & * & \overline{\Psi}_{44} & 0 & \overline{\Psi}_{46} & 0 & 0\\ & * & * & * & \overline{\Psi}_{55} & 0 & 0 & 0\\ & * & * & * & * & \overline{\Psi}_{66} & 0 & 0\\ & * & * & * & * & * & -\rho I & 0\\ & * & * & * & * & * & * & -\rho I\end{bmatrix},$$

$$\overline{\Theta}(i)=\begin{bmatrix}\overline{\Theta}_{11}(i) & \overline{\Theta}_{12}(i) & \overline{\Theta}_{13}(i) & \overline{\Theta}_{14} & \overline{\Theta}_{15}(i) & E_i & \overline{Y}F_i^T\\ & \overline{\Theta}_{22} & \overline{\Theta}_{23}(i) & \overline{\Theta}_{24} & \overline{\Theta}_{25}(i) & \varepsilon_1E_i & 0\\ & * & \overline{\Theta}_{33}(i) & \overline{\Theta}_{34} & \overline{\Theta}_{35}(i) & \varepsilon_2E_i & 0\\ & * & * & \overline{\Theta}_{44} & 0 & 0 & 0\\ & * & * & * & \overline{\Theta}_{55} & 0 & 0\\ & * & * & * & * & -\rho I & 0\\ & * & * & * & * & * & -\rho I\end{bmatrix},$$

$$\overline{\Phi}(i)=\begin{bmatrix}\overline{\Phi}_{11}(i) & \overline{\Phi}_{12}(i) & \overline{\Phi}_{13}(i) & \overline{\Phi}_{14}(i) & E_i & \overline{Y}F_i^T\\ & \overline{\Phi}_{22} & \overline{\Phi}_{23}(i) & \overline{\Phi}_{24}(i) & \varepsilon_1E_i & 0\\ & * & \overline{\Phi}_{33}(i) & 0 & 0 & 0\\ & * & * & \overline{\Phi}_{44} & 0 & 0\\ & * & * & * & -\rho I & 0\\ & * & * & * & * & -\rho I\end{bmatrix},$$

$$\overline{\Xi}(i)=\begin{bmatrix}\overline{P}_i+d\mathcal{S}\left(\frac{\overline{H}_1}{2}\right) & -d\overline{H}_1+d\overline{H}_2 & d\overline{H}_3\\ & -d\mathcal{S}\left(\overline{H}_2-\frac{\overline{H}_1}{2}\right) & d\overline{H}_4\\ & * & d\mathcal{S}\left(\frac{\overline{H}_5}{2}\right)\end{bmatrix},$$

$$\tilde{Y}_1=\left[\overline{Y}^T,\ 0,\ 0,\ 0,\ 0,\ 0,\ 0,\ 0\right]^T,$$
$$\tilde{Y}_2=\left[\overline{Y}^T,\ 0,\ 0,\ 0,\ 0,\ 0,\ 0\right]^T,$$
$$\tilde{Y}_3=\left[\overline{Y}^T,\ 0,\ 0,\ 0,\ 0,\ 0\right]^T,$$
$$\tilde{Y}_4=\left[\overline{Y}^T,\ 0,\ 0,\ 0\right]^T,$$
$$\overline{\Psi}_{11}(i)=\textstyle\sum_{j=1}^{N}\lambda_{ij}^{*}\overline{P}_j+2\alpha\overline{P}_i+\mathcal{S}\left(-\frac{\overline{H}_1}{2}+\overline{G}_1+A_i\overline{Y}^T\right),$$
$$\overline{\Psi}_{12}(i)=\overline{P}_i+\overline{G}_2-\overline{Y}^T+\varepsilon_1\overline{Y}A_i^T,$$
$$\overline{\Psi}_{13}(i)=\overline{H}_1-\overline{H}_2+\overline{G}_3-\overline{G}_1^T+B_i\overline{K}_i+\varepsilon_2\overline{Y}A_i^T,$$
$$\overline{\Psi}_{14}=-\overline{H}_3+\overline{G}_4,\ \overline{\Psi}_{15}(i)=C_i-\overline{Y}\mathrm{Y}_2,\ \overline{\Psi}_{16}=\sqrt{d}\overline{G}_1^T,$$
$$\overline{\Psi}_{22}=-\mathcal{S}\left(\varepsilon_1\overline{Y}^T\right),\ \overline{\Psi}_{23}(i)=-\overline{G}_2^T-\varepsilon_2\overline{Y}^T+\varepsilon_1B_i\overline{K}_i,$$
$$\overline{\Psi}_{25}(i)=\overline{\Theta}_{25}(i)=\overline{\Phi}_{24}(i)=\varepsilon_1C_i,\ \overline{\Psi}_{26}=\sqrt{d}\overline{G}_2^T,$$
$$\overline{\Psi}_{33}(i)=\mathcal{S}\left(\overline{H}_2-\frac{\overline{H}_1}{2}-\overline{G}_3+\varepsilon_2B_i\overline{K}_i\right)-de^{-2\alpha d}\overline{Q}_3,$$
$$\overline{\Psi}_{34}=-\overline{H}_4-e^{-2\alpha d}\overline{Q}_2^T-\overline{G}_4,\ \overline{\Psi}_{35}(i)=\overline{\Theta}_{35}(i)=\varepsilon_2C_i,\ \overline{\Psi}_{36}=\sqrt{d}\overline{G}_3^T,$$
$$\overline{\Psi}_{44}=-\mathcal{S}\left(\frac{\overline{H}_5}{2}\right)-\frac{e^{-2\alpha d}}{d}\overline{Q}_1,\ \overline{\Psi}_{46}=\sqrt{d}\overline{G}_4^T,$$
$$\overline{\Psi}_{55}=-\mathrm{Y}_3,\ \overline{\Psi}_{66}=-e^{-2\alpha d}\overline{U},$$
$$\overline{\Phi}_{11}(i)=\textstyle\sum_{v=1,j}^{N}\lambda_{ij}^{*}\overline{P}_j+2\alpha\overline{P}_i+\sigma\overline{\Lambda}_i+\mathcal{S}\left(A_i\overline{Y}^T+B_i\overline{K}_i\right),$$
$$\overline{\Phi}_{12}(i)=\overline{P}_i-\overline{Y}+\varepsilon_1\overline{Y}A_i^T+\left(\varepsilon_1B_i\overline{K}_i\right)^T,$$
$$\overline{\Phi}_{13}(i)=B_i\overline{K}_i,\ \overline{\Phi}_{14}(i)=C_i-\overline{Y}\mathrm{Y}_2,$$
$$\overline{\Phi}_{22}=\mathcal{S}\left(-\varepsilon_1\overline{Y}^T\right),\ \overline{\Phi}_{23}(i)=\varepsilon_1B_i\overline{K}_i,$$
$$\overline{\Phi}_{33}(i)=-\overline{\Lambda}_i,\ \overline{\Phi}_{44}=\delta I-\mathrm{Y}_3,$$

$$
\begin{aligned}
\overline{\Theta}_{11}(i) &= \overline{\Psi}_{11}(i) + \alpha d\mathcal{S}\big(\overline{H}_1\big) + d\mathcal{S}\big(\overline{H}_3\big) + d\overline{Q}_1, \overline{\Theta}_{12}(i) = \overline{\Psi}_{12}(i) + d\tfrac{\mathcal{S}(\overline{H}_1)}{2},\\
\overline{\Theta}_{13}(i) &= \overline{\Psi}_{13}(i) + 2\alpha d(H_2 - H_1) + dH_4^T + d\overline{Q}_2,\\
\overline{\Theta}_{14} &= \overline{\Psi}_{14} + 2\alpha d\overline{H}_3 + d\tfrac{\mathcal{S}(\overline{H}_5)}{2}, \overline{\Theta}_{15}(i) = C_i - \overline{Y}\mathrm{Y}_2,\\
\overline{\Theta}_{22} &= \overline{\Psi}_{22} + d\overline{U}, \overline{\Theta}_{23}(i) = \overline{\Psi}_{23}(i) + d\big(\overline{H}_2 - \overline{H}_1\big),\\
\overline{\Theta}_{24} &= d\overline{H}_3,\\
\overline{\Theta}_{33}(i) &= \mathcal{S}\Big(\overline{H}_2 - \tfrac{\overline{H}_1}{2} - \overline{G}_3 + \varepsilon_2 B_i\overline{K}_i\Big) + 2\alpha d\mathcal{S}\Big(-\overline{H}_2 + \tfrac{\overline{H}_1}{2}\Big) + d\overline{Q}_3,\\
\overline{\Theta}_{34} &= \overline{\Psi}_{34} + 2\alpha d\overline{H}_4,\\
\overline{\Theta}_{44} &= \overline{\Psi}_{44} + \alpha d\mathcal{S}\big(\overline{H}_5\big), \overline{\Theta}_{55} = -\mathrm{Y}_3, \lambda_{ij}^* = \mathcal{E}\big\{\lambda_{ij}(\iota)\big\}.
\end{aligned}
$$

Then, the extended dissipativity stabilization of semi-MSS (1) can be achieved by event-triggered controller (5) with feedback-gain and event-triggered matrices

$$K_i = \bar{K}_i(\bar{Y}^T)^{-1},\ \Lambda_i = \bar{Y}^{-1}\bar{\Lambda}_i(\bar{Y}^T)^{-1}. \tag{35}$$

Proof. In the light of (2), we can rewrite (9) as

$$
\begin{bmatrix}
\Psi_{11}^{\diamond}(i) & \Psi_{12}^{\diamond}(i) & \Psi_{13}^{\diamond}(i) & \Psi_{14} & \Psi_{15}(i) & \Psi_{16}\\
* & \Psi_{22} & \Psi_{23}(i) & 0 & \Psi_{25}(i) & \Psi_{26}\\
* & * & \Psi_{33}(i) & \Psi_{34} & \Psi_{35}(i) & \Psi_{36}\\
* & * & * & \Psi_{44} & 0 & \Psi_{46}\\
* & * & * & * & \Psi_{55} & 0\\
* & * & * & * & * & \Psi_{66}
\end{bmatrix}
+
\begin{bmatrix} YE_i\\ \varepsilon_1 YE_i\\ \varepsilon_2 YE_i\\ 0\\ 0\\ 0 \end{bmatrix}
\Delta(t)
\begin{bmatrix} F_i^T\\ 0\\ 0\\ 0\\ 0\\ 0 \end{bmatrix}^T
+
\begin{bmatrix} F_i^T\\ 0\\ 0\\ 0\\ 0\\ 0 \end{bmatrix}
\Delta^T(t)
\begin{bmatrix} YE_i\\ \varepsilon_1 YE_i\\ \varepsilon_2 YE_i\\ 0\\ 0\\ 0 \end{bmatrix}^T
< 0, \tag{36}
$$

where

$$
\begin{aligned}
\Psi_{11}^{\diamond}(i) &= \sum_{j=1}^{N}\lambda_{ij}^* P_j + 2\alpha P_i + \mathcal{S}(-\frac{H_1}{2} + G_1 + A_i Y),\\
\Psi_{12}^{\diamond}(i) &= P_i + G_2 - Y + \varepsilon_1 YA_i^T,\\
\Psi_{13}^{\diamond}(i) &= H_1 - H_2 + G_3 - G_1^T + B_i K_i + \varepsilon_2 YA_i^T.
\end{aligned}
$$

Using Lemma 2, (36) is equivalent to

$$
\begin{bmatrix}
\Psi_{11}^{\diamond}(i) & \Psi_{12}^{\diamond}(i) & \Psi_{13}^{\diamond}(i) & \Psi_{14} & \Psi_{15}(i) & \Psi_{16}\\
* & \Psi_{22} & \Psi_{23}(i) & 0 & \Psi_{25}(i) & \Psi_{26}\\
* & * & \Psi_{33}(i) & \Psi_{34} & \Psi_{35}(i) & \Psi_{36}\\
* & * & * & \Psi_{44} & 0 & \Psi_{46}\\
* & * & * & * & \Psi_{55} & 0\\
* & * & * & * & * & \Psi_{66}
\end{bmatrix}
+ \frac{1}{\rho}
\begin{bmatrix} YE_i\\ \varepsilon_1 YE_i\\ \varepsilon_2 YE_i\\ 0\\ 0\\ 0 \end{bmatrix}
\begin{bmatrix} Y^T E_i\\ \varepsilon_1 Y^T E_i\\ \varepsilon_2 Y^T E_i\\ 0\\ 0\\ 0 \end{bmatrix}^T
+ \rho
\begin{bmatrix} F_i^T\\ 0\\ 0\\ 0\\ 0\\ 0 \end{bmatrix}
\begin{bmatrix} F_i^T\\ 0\\ 0\\ 0\\ 0\\ 0 \end{bmatrix}^T
< 0,
$$

which, according to Schur's complement, can be further equivalently transformed into

$$
\Gamma_1(i) = \begin{bmatrix}
\overline{\Psi}_{11}^{\diamond}(i) & \Psi_{12}^{\diamond}(i) & \Psi_{13}^{\diamond}(i) & \Psi_{14} & \Psi_{15}(i) & \Psi_{16} & YE_i\\
* & \Psi_{22} & \Psi_{23}(i) & 0 & \Psi_{25}(i) & \Psi_{26} & \varepsilon_1 YE_i\\
* & * & \Psi_{33}(i) & \Psi_{34} & \Psi_{35}(i) & \Psi_{36} & \varepsilon_2 YE_i\\
* & * & * & \Psi_{44} & 0 & \Psi_{46} & 0\\
* & * & * & * & \Psi_{55} & 0 & 0\\
* & * & * & * & * & \Psi_{66} & 0\\
* & * & * & * & * & * & -\rho I
\end{bmatrix} < 0, \tag{37}
$$

where

$$
\bar{\Psi}_{11}^{\diamond}(i) = \sum_{j=1}^{N}\lambda_{ij}^* P_j + 2\alpha P_i + \mathcal{S}(-\frac{H_1}{2} + G_1 + A_i Y) + \rho F_i^T F_i.
$$

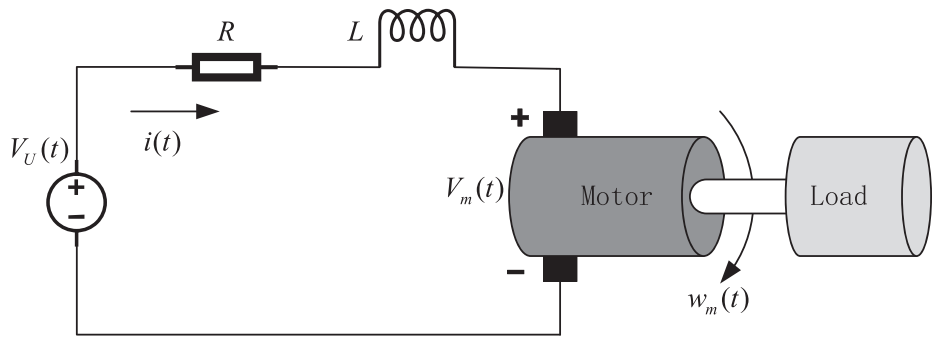

Fig. 1. The DC motor device.

From (9) we know that Y is an invertible matrix. Set $\bar{Y} = Y^{-1}$. Then, (37) can be guaranteed by

$$diag\{\bar{Y},\ \bar{Y},\ \bar{Y},\ \bar{Y},\ I,\ \bar{Y},\ I,\ I\}\ \Gamma(i)\ diag\{\bar{Y}^T,\ \bar{Y}^T,\ \bar{Y}^T,\ \bar{Y}^T,\ I,\ \bar{Y}^T,\ I,\ I\} < 0. \tag{38}$$

By (35), we can obtain $\bar{K}_i = K_i\bar{Y}^T$ and $\bar{\Lambda}_i = \bar{Y}\Lambda_i\bar{Y}^T$. Set further

$$\bar{U} = \bar{Y}U\bar{Y}^T, \bar{P}_i = \bar{Y}P_i\bar{Y}^T,\ \bar{Q}_z = \bar{Y}Q_z\bar{Y}^T\ \ (z = 1, 2, 3),$$
$$\bar{G}_n = \bar{Y}G_n\bar{Y}^T\ \ (n = 1, 2, 3, 4),\ \bar{H}_m = \bar{Y}H_m\bar{Y}^T\ \ (m = 1, 2, 3, 4, 5).$$

Then, (38) can be rewritten as $\bar{\Psi}(i) < 0$ when $\Upsilon_1 = 0$. In the case when $\Upsilon_1 < 0$, (38) can be equivalently transformed into $\begin{bmatrix} \bar{\Psi}(i) & \bar{\Upsilon}_1 \\ * & \Upsilon_1^{-1} \end{bmatrix} < 0$ by using Schur's complement again. In this way, we have shown that (30) implies (9). In a similar way to the proof above, we can prove that (31)–(34) imply (10)–(13), respectively, and we complete the proof. □

Remark 6. The theorem gives an efficient method for solving the extended dissipativity stabilization issue. Based on the analysis result in Theorem 1 and some equivalent transformations of matrix inequalities, a condition is developed in the form of a set of LMIs, which can be readily verified by available MATLAB YALMIP or LMI toolbox. When the condition holds true, the needed feedback-gain and event-triggered matrices are able to be achieved simultaneously.

4. Numerical examples

We use the DC model in [36,37] and the robot arm model in [38] to illustrate the validity of the designed MDSETM-based controller.

Example 1. The DC motor model of [36,37], depicted in Fig. 1, can be characterized as

$$\begin{cases} V_m(t) = K_b w_m(t), \\ V_U(t) = L\frac{di(t)}{dt} + Ri(t) + V_m(t), \\ T(t) = K_m i(t), \\ J_m\frac{dw_m(t)}{dt} = -K_f w_m(t) + T(t), \end{cases}$$

where $V_m(t)$ denotes the electrical voltage, K_b is a scalar corresponding to certain physical properties, $w_m(t)$ represents the angular velocity of the load, L and R, respectively, means the inductance and the resistance, $i(t)$ represents the current, $T(t)$ denotes the torque at the DC motor shaft, K_m stands for the armature constant, J_m is the inertial load, and $K_f w_m(t)$ represents a linear approximation of the viscous friction.

After some computation, the DC motor model can be expressed as

$$\dot{x}(t) = (A_i + \Delta A_i)x(t) + B_i u(t) + C_i\varpi(t),$$

where $i \in \{1, 2, 3\}$, $x(t) = [w_m(t),\ i(t)]^T$ and

$$A_i = \begin{bmatrix} a_i^{11} & a_i^{12} \\ a_i^{21} & a_i^{22} \end{bmatrix},\ B_i = \begin{bmatrix} b_i^{11} & 0 \\ 0 & b_i^{22} \end{bmatrix}.$$

As in [36,37], the motor has three modes, namely normal, low, and medium modes; parameters a_i^{11}, a_i^{12}, a_i^{21}, a_i^{22}, b_i^{11}, and b_i^{22} are presented in Table 1; the other mode-dependent parameters are listed below:

$$E_1 = E_2 = E_3 = \begin{bmatrix} 0.1 \\ 0.1 \end{bmatrix},\ F_1 = F_2 = F_3 = \begin{bmatrix} 0.1 & 0.1 \end{bmatrix},$$

Table 1
Parameters of the DC motor.

Mode	a_i^{11}	a_i^{12}	a_i^{21}	a_i^{22}	b_i^{11}	b_i^{22}
i=1	-0.479908	5.1546	-3.81625	14.4723	5.8705212	15.50107
i=2	-1.60261	9.1632	-0.5918697	3.0317	10.285129	2.2282663
i=3	0.634617	0.917836	-0.50569	2.48116	0.7874647	1.5302844

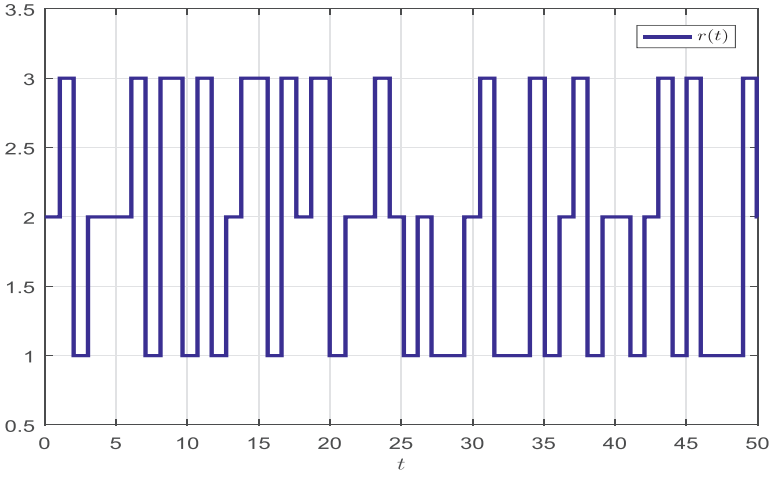

Fig. 2. The switching signal of Example 1.

$$C_1 = \begin{bmatrix} 0.1 & 0 \\ 0.1 & 0.1 \end{bmatrix}, C_2 = \begin{bmatrix} 0.12 & 0.1 \\ 0 & 0.1 \end{bmatrix}, C_3 = \begin{bmatrix} 0.1 & 0 \\ 0 & 0.14 \end{bmatrix}.$$

Note that $(\bar{A}_1, B_1)$, $(\bar{A}_2, B_2)$ and $(\bar{A}_3, B_3)$ are controllable. Suppose that the switching is subjected to a semi-Markov process, where the sojourn time obeys the Weibull distribution when $i = 1, 2$ and the exponential distribution when $i = 3$. To be more specific, we choose transition rate function $\lambda_i(\iota) = (\beta_2/\beta_1{}^{\beta_2})\iota^{\beta_2 - 1}$ for mode i, in which β_1 and β_2 are the scale and shape parameters, respectively. Herein, we set $\beta_1 = 1$ and $\beta_2 = 2$ for $i = 1$ and $\beta_1 = 1$ and $\beta_2 = 3$ for $i = 2$, and exponential distribution with parameter 0.5. The transition rate intensity q_{ij} is chosen as

$$q_{ij} = \begin{bmatrix} 0 & 0.5 & 0.5 \\ 0.2 & 0 & 0.8 \\ 0.8 & 0.2 & 0 \end{bmatrix}.$$

Correspondingly, we have

$$\mathcal{E}\{\lambda(\iota)\} = \begin{bmatrix} -3.545 & 1.7725 & 1.7725 \\ 1.0833 & -5.4164 & 4.3332 \\ 3.2 & 0.8 & -4 \end{bmatrix}.$$

Set $\alpha = 0.1, \delta = 0.1, d = 0.05, \sigma = 0.01, \varepsilon_1 = 0.03, \varepsilon_2 = 0.01$, the external disturbance $\varpi(t) = \left[e^{-t}, e^{-t}\right]^T$, and the initial condition $x(0) = [0; 0]$. The mode switching process is depicted in Fig. 2.

Next, consider the following four cases:

Case 1. $\mathscr{H}_\infty$ **performance**

Choose $\Upsilon_1 = -I$, $\Upsilon_2 = 0$, $\Upsilon_3 = 5^2 I$, and $\Upsilon_4 = 0$. Then, by solving LMIs (30)–(34) in Theorem 2 via the SeDuMi solver under the YALMIP interface in MATLAB, we can obtain

$$K_1 = \begin{bmatrix} -0.7523 & -0.3702 \\ 0.2026 & -1.5200 \end{bmatrix}, K_2 = \begin{bmatrix} -0.3678 & -0.3307 \\ 0.4398 & -6.5651 \end{bmatrix}, K_3 = \begin{bmatrix} -5.8111 & -1.7759 \\ 0.7931 & -9.4983 \end{bmatrix},$$

$$\Lambda_1 = \begin{bmatrix} 3.3904 & -6.1099 \\ -6.1099 & 42.1919 \end{bmatrix}, \Lambda_2 = \begin{bmatrix} 2.4372 & -1.6619 \\ -1.6619 & 22.7854 \end{bmatrix}, \Lambda_3 = \begin{bmatrix} 2.7637 & -2.1649 \\ -2.1649 & 22.4972 \end{bmatrix}.$$

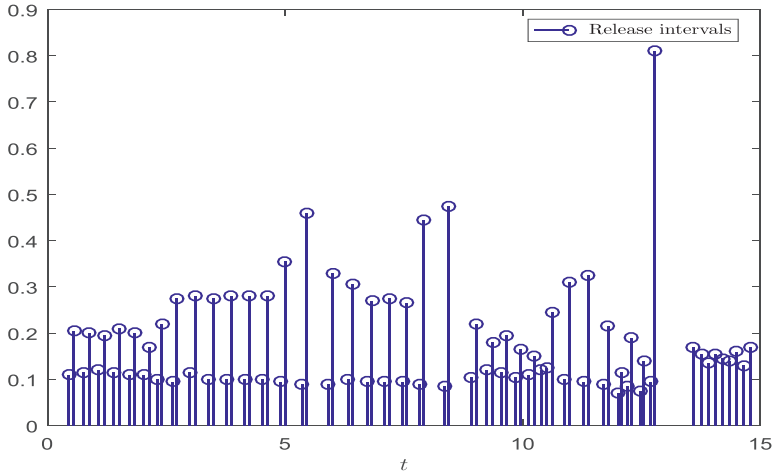

Fig. 3. Release intervals and instants of the MDSETM in Case 1 of Example 1.

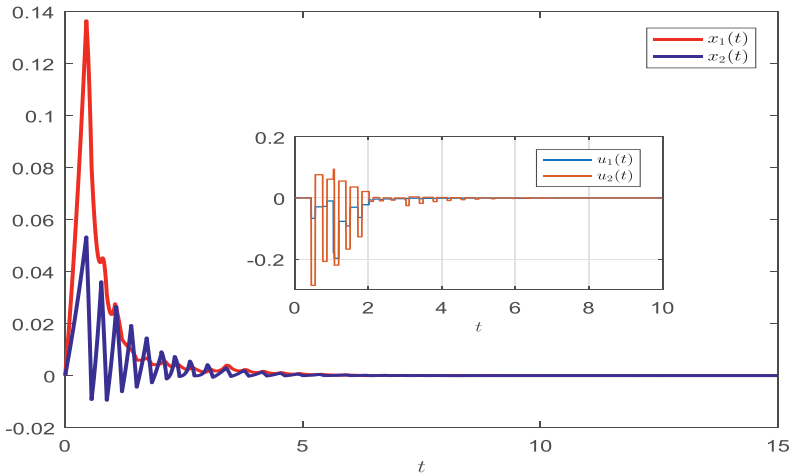

Fig. 4. State trajectories with control in Case 1 of Example 1.

Table 2
Comparison of the NTEs under different ETMs in Case 1 of Example 1.

Mechanism	The NTEs	Transmission rate (%)
PSM in [45]	300	100
STEM in [29]	175	58
STEM in [44]	97	32
MDSETM	82	27

Figure 3 depicts the event-triggered release intervals and instants based on the proposed MDSETM. Figure 4 exhibits state trajectories of the SCLS. We can find that the system achieves stability under the designed MDSETM-based controller. Define

$$\bar{H}(t) = \frac{\int_0^t x^T(\mu)x(\mu)d\mu}{\int_0^t \varpi^T(\mu)\varpi(\mu)d\mu},$$

which corresponds to the square of the $\mathscr{H}_\infty$ performance index when $t \to \infty$. Then, the evolution of $\bar{H}(t)$ with the zero-initial condition is depicted in Fig. 5. It is found that $\bar{H}(t)$ converges eventually to 0.0112, which is less than predefined $\mathscr{H}_\infty$ performance level. Hence, the simulations confirm the validity of the present the MDSETM-based control method for Case 1.

Table 2 provides a comparison of the NTEs under different ETMs. As shown in the table, the NTEs based on the present the MDSETM is 73% less than that based on the PSM in [45], 31% less than that based on the STEM in [29], and 5% less than that based on the STEM in [44].

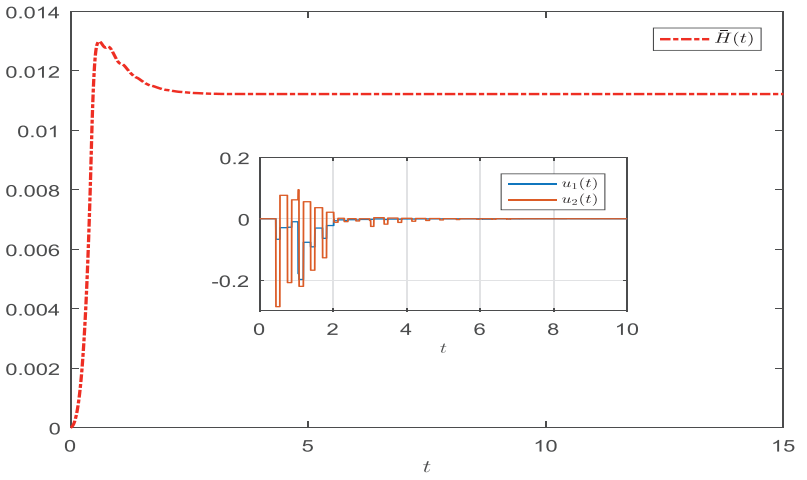

Fig. 5. The trajectory of $\bar{H}(t)$.

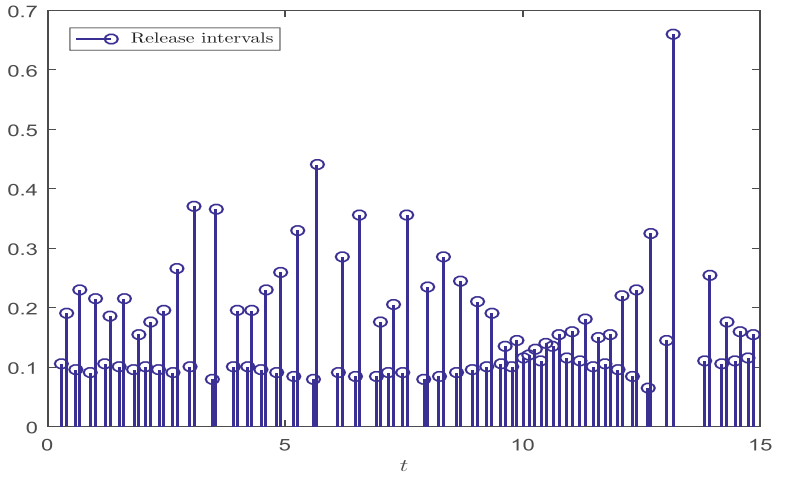

Fig. 6. Release intervals and instants of the MDSETM in Case 2 of Example 1.

Case 2. $\mathscr{L}_2 - \mathscr{L}_\infty$ performance

Choose $\Upsilon_1 = 0$, $\Upsilon_2 = 0$, $\Upsilon_3 = 5.7^2 I$, and $\Upsilon_4 = I$. Then, by solving LMIs (30)–(34) in Theorem 2 via the SeDuMi solver under the YALMIP interface in MATLAB, we can obtain

$$K_1 = \begin{bmatrix} -1.4077 & -0.4561 \\ 0.1076 & -1.5815 \end{bmatrix}, K_2 = \begin{bmatrix} -0.7761 & -0.3625 \\ 0.1683 & -7.3356 \end{bmatrix}, K_3 = \begin{bmatrix} -10.9131 & -1.3435 \\ 0.4508 & -10.4965 \end{bmatrix},$$

$$\Lambda_1 = \begin{bmatrix} 14.0691 & -5.8641 \\ -5.8641 & 67.3342 \end{bmatrix}, \Lambda_2 = \begin{bmatrix} 13.3064 & -1.3169 \\ -1.3169 & 43.2120 \end{bmatrix}, \Lambda_3 = \begin{bmatrix} 13.5803 & -2.6019 \\ -2.6019 & 41.1622 \end{bmatrix}.$$

Figure 6 depicts the event-triggered release intervals and instants based on the proposed mechanism. Figure 7 exhibits state trajectories of the SCLS. We can find that the system achieves stability under the designed MDSETM-based controller. Define

$$\bar{L}(t) = \frac{\sup_{t\geq 0} x^T(t)x(t)}{\int_0^t \varpi^T(\mu)\varpi(\mu)d\mu},$$

which corresponds to the square of the $\mathscr{L}_2 - \mathscr{L}_\infty$ performance index when $t \to \infty$. Then, the trajectory of $\bar{L}(t)$ with the zero-initial condition is depicted in Fig. 8. It is found that $\bar{L}(t)$ converges eventually to 0, which is less than predefined $\mathscr{L}_2 - \mathscr{L}_\infty$ performance level. Hence, the simulations confirm the validity of the present the MDSETM-based control method for Case 2.

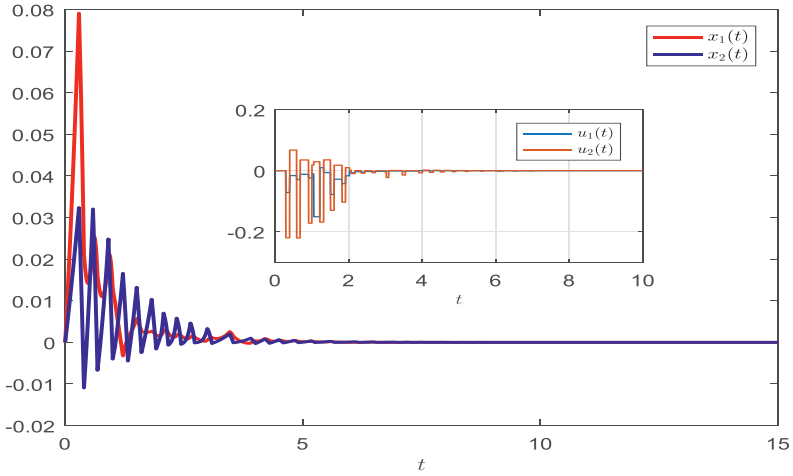

Fig. 7. State trajectories with control in Case 2 of Example 1.

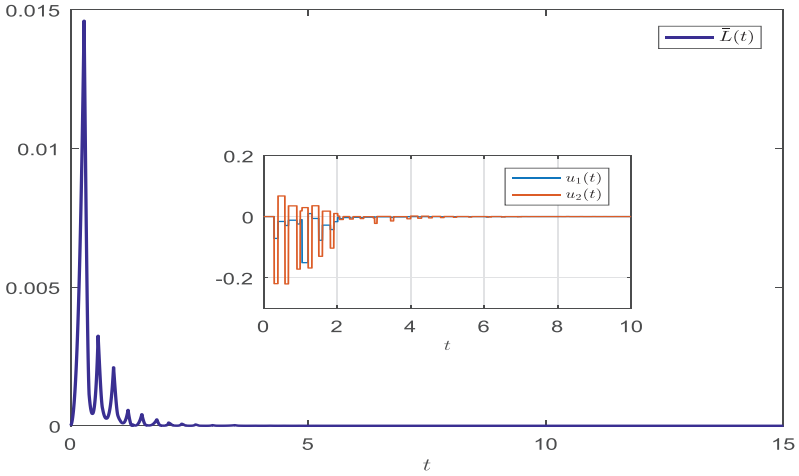

Fig. 8. The trajectory of $\bar{L}(t)$.

Table 3
Comparison of the NTEs under different ETMs in Case 2 of Example 1 .

Mechanism	The NTEs	Transmission rate (%)
PSM in [45]	300	100
STEM in [29]	169	56
STEM in [44]	102	34
MDSETM	91	30

Table 3 provides a comparison of the NTEs under different ETMs. As shown in the table, the NTEs based on the present the MDSETM is 70% less than that based on the periodic sampling mechanism (PSM) in [45], 26% less than that based on the STEM in [29], and 4% less than that based on the STEM in [44].

Cases 3 and 4. Passive and $(\mathscr{Q}, \mathscr{S}, \mathscr{R})$ - dissipative performances

Choose $\Upsilon_1 = 0$, $\Upsilon_2 = I$, $\Upsilon_3 = 4.8^2 I$, $\Upsilon_4 = 0$ and $\Upsilon_1 = -I$, $\Upsilon_2 = I$, $\Upsilon_3 = 3.8I$, $\Upsilon_4 = 0$, respectively. Solve LMIs (30)–(34) in Theorem 2 resulting in

$$K_1 = \begin{bmatrix} -0.3385 & 0.0466 \\ 0.2724 & -1.4282 \end{bmatrix}, K_2 = \begin{bmatrix} -0.1315 & -0.2545 \\ 0.8227 & -5.6482 \end{bmatrix}, K_3 = \begin{bmatrix} -2.6193 & 0.0299 \\ 1.3239 & -8.4859 \end{bmatrix},$$

$$\Lambda_1 = \begin{bmatrix} 1.0529 & -4.0905 \\ -4.0905 & 20.6529 \end{bmatrix}, \Lambda_2 = \begin{bmatrix} 0.4534 & -1.5255 \\ -1.5255 & 9.8624 \end{bmatrix}, \Lambda_3 = \begin{bmatrix} 0.4981 & -1.5898 \\ -1.5898 & 9.7622 \end{bmatrix}.$$

for passivity and

$$K_1 = \begin{bmatrix} -0.4663 & -0.1464 \\ 0.2571 & -1.4668 \end{bmatrix}, K_2 = \begin{bmatrix} -0.2110 & -0.2558 \\ 0.8027 & -6.1568 \end{bmatrix}, K_3 = \begin{bmatrix} -3.6713 & -0.6374 \\ 1.2489 & -9.0364 \end{bmatrix},$$

$$\Lambda_1 = \begin{bmatrix} 11.2148 & -36.5103 \\ -36.5103 & 196.7065 \end{bmatrix}, \Lambda_2 = \begin{bmatrix} 6.1781 & -14.7566 \\ -14.7566 & 104.6375 \end{bmatrix}, \Lambda_3 = \begin{bmatrix} 6.7317 & -15.2888 \\ -15.2888 & 101.5738 \end{bmatrix}.$$

for $(\mathscr{Q}, \mathscr{S}, \mathscr{R})$ - dissipativity. Based on the above feedback-gain and event-triggered matrices, the expected performances of the SCLS can be guaranteed. The simulations are omitted for the sake of brevity.

Example 2. Consider the 2-degree-of-freedom (2-DOF) robot arm model in [38]. The dynamics of the model is given by

$$F(\vartheta) + M(\vartheta)\ddot{\vartheta} + N(\vartheta, \dot{\vartheta})\dot{\vartheta} = \tau^*, \tag{39}$$

where $F(\vartheta)$, $M(\vartheta)$, and $N(\vartheta, \dot{\vartheta})$ denote the gravity term, the mass matrix, and the Coriolis and centrifugal term, respectively. To be more specific,

$$\vartheta = [\vartheta_1, \ \vartheta_2]^T, M(\vartheta) = \begin{bmatrix} M_{11}(\vartheta) & M_{12}(\vartheta) \\ M_{21}(\vartheta) & M_{22}(\vartheta) \end{bmatrix},$$

$$F(\vartheta) = \begin{bmatrix} F_1(\vartheta) \\ F_2(\vartheta) \end{bmatrix}, N(\vartheta, \dot{\vartheta}) = \begin{bmatrix} N_1(\vartheta, \dot{\vartheta}) \\ N_2(\vartheta, \dot{\vartheta}) \end{bmatrix}$$

with

$$\begin{aligned} M_{11}(\vartheta) &= m_1 f_1^2 + m_2(f_1^2 + 2f_1 f_2 \cos\vartheta_2 + f_2^2), \\ M_{12}(\vartheta) &= m_2(f_1 f_2 \cos\vartheta_2) + f_2^2, \\ M_{21}(\vartheta) &= M_{12}(\vartheta), \ M_{22}(\vartheta) = m_2 f_2^2, \\ N_1(\vartheta, \dot{\vartheta}) &= -m_2(f_1 f_2 \sin\vartheta_2(2\dot{\vartheta}_1\dot{\vartheta}_2 + \dot{\vartheta}_2^2)), \\ N_2(\vartheta, \dot{\vartheta}) &= m_2 f_1 f_2 \dot{\vartheta}_1^2 \sin\vartheta_2, \\ F_1(\vartheta) &= (m_1 + m_2) f_1 g \cos\vartheta_1 + m_2 g f_2 \cos(\vartheta_1 + \vartheta_2), \\ F_2(\vartheta) &= m_2 g f_2 \cos(\vartheta_1 + \vartheta_2). \end{aligned}$$

Considering parametric uncertainty and extend disturbance, the linear model of (39) can be described by

$$\dot{x}(t) = (A_i + \Delta A_i)x(t) + B_i u(t) + C_i \varpi(t),$$

where

$$\dot{x} = \left[\vartheta_1, \ \vartheta_2, \ \dot{\vartheta}_1, \ \dot{\vartheta}_2\right]^T, \ u(t) = \tau^*,$$

$$A_1 = \begin{bmatrix} 0 & 0 & 1 & 0 \\ 0 & 0 & 0 & 1 \\ a(i)_1 & a(i)_2 & 0 & 0 \\ a(i)_3 & a(i)_4 & 0 & 0 \end{bmatrix}, \ B_i = \begin{bmatrix} b_i^1 & b(i)_2 \\ b_i^3 & b_i^4 \end{bmatrix}$$

with

$$\begin{aligned} a(i)_1 = &-\frac{g f_2 m_{2i}(m_{1i} f_1^2 + f_1^2 m_{2i} + m_{2i} f_2^2 + 2 f_1 f_2 m_{2i})}{m_{1i} f_1^2 m_{2i} f_2^2} \\ &- \frac{g f_2 m_{2i}(f_1 + f_2)(m_{1i} f_1 + f_1 m_{2i} + m_{2i} f_2)}{m_{1i} f_1^2 m_{2i} f_2^2}, \\ a(i)_2 = &-\frac{g f_2 m_{2i}(m_{1i} f_1^2 + f_1^2 m_{2i} + m_{2i} f_2^2 + 2 f_1 f_2 m_{2i})}{m_{1i} f_1^2 m_{2i} f_2^2} \\ &- \frac{g m_{2i}^2 f_2^2 (f_1 + f_2)}{m_{1i} f_1^2 m_{2i} f_2^2}, \end{aligned}$$

$$a(i)_3 = \frac{g(f_2 + f_1 m_{2i})}{m_{1i} f_1^2 - m_{2i} f_2^2 g(f_1 m_{1i} + f_1 m_{2i} + f_2 m_{2i})},$$

$$a(i)_4 = \frac{g(f_2 + f_1 m_{2i})}{m_{1i} f_1^2 - g f_2 m_{2i} f_2^2 m_{2i}},$$

$$b(i)_1 = \frac{f_1 + f_2}{f_2 m_{1i} f_1^2},$$

$$b(i)_2 = \frac{m_{1i} f_1^2 + f_1^2 m_{2i} + m_{2i} f_2^2 + 2 f_1 l_2 m_{2i}}{m_{1i} f_1^2 m_{2i} f_2^2}$$

$$b(i)_3 = m_{2i} f_2^2,$$

$$b(i)_4 = -\frac{f_2 + f_1 m_{2i}}{m_{1i} f_1^2 m_{2i} f_2^2},$$

$$Z_{11} = m_{11} f_1^2,\ Z_{21} = m_{21} f_1^2,\ Z_{12} = m_{12} f_2^2,\ Z_{22} = m_{22} f_2^2.$$

The following parameters are taken from [38]:

$$g = 9.8 m/s^2,\ f_1 = 0.4m,\ f_2 = 0.2m,$$

$$Z_{11} = 0.25N * m,\ Z_{21} = 0.1N * m,$$

$$Z_{12} = 0.4N * m,\ Z_{22} = 0.2N * m,$$

$$m_{11} = 0.5kg,\ m_{21} = 0.3kg,$$

$$m_{12} = 0.8kg,\ m_{22} = 0.5kg.$$

The switch between different speeds depends on $\{\varsigma(t), t \geq 0\}$ taking values in $\bar{N} = \{1, 2\}$. The other parameters are taken as follows:

$$C_1 = \begin{bmatrix} -0.5 & 0 & 0 & 0 \\ 0 & 1 & -1 & 0 \\ 0 & 0 & -1 & 0 \\ 0 & 0 & 0 & 0.5 \end{bmatrix},\ C_2 = \begin{bmatrix} -1.8 & 0 & 0 & 0 \\ 0 & 0.3 & 0 & 0.1 \\ 0 & 0 & 0.3 & 0 \\ 0 & 0 & 0 & 0.8 \end{bmatrix}.$$

We assume that the sojourn time follows the Weibull distribution. To be more specific, we choose transition rate function $\lambda_i(\iota) = (\beta_2/\beta_1^{\beta_2})\iota^{\beta_2 - 1}$ for mode i, in which β_1 and β_2 are the scale and shape parameters, respectively. Herein, we set $\beta_1 = 1$ and $\beta_2 = 2$ for $i = 1$ and $\beta_1 = 1$ and $\beta_2 = 3$ for $i = 2$, which implies that

$$\left(\lambda_{ij}(\iota)\right)_{2\times 2} = \begin{bmatrix} -2\iota & 2\iota \\ 3\iota^2 & -3\iota^2 \end{bmatrix}.$$

Correspondingly, we have

$$\mathcal{E}\{\lambda(\iota)\} = \begin{bmatrix} -1.7725 & 1.7725 \\ 2.7082 & -2.7082 \end{bmatrix}.$$

We set $\alpha = 0.1, \delta = 0.1, d = 0.05, \sigma = 0.001, \varepsilon_1 = 0.03, \varepsilon_2 = 0.01$, the external disturbance $\varpi(t) = \left[5e^{-t}, 10e^{-t}, 10e^{-t}, 10e^{-t}\right]^T$, and the initial condition $x(0) = \left[-\frac{\pi}{2}; -\frac{\pi}{2}; 0; 0\right]$. The mode switching is exhibited in Fig. 9. In what follows, for brevity, we only consider two cases of the extended dissipativity.

Case 1. Passvie performance

Choose $\Upsilon_1 = 0$, $\Upsilon_2 = I$, $\Upsilon_3 = 6.5^2 I$, and $\Upsilon_4 = 0$. Then, by solving LMIs (30)–(34) in Theorem 2 via the SeDuMi solver under the YALMIP interface in MATLAB, we can obtain

$$K_1 = \begin{bmatrix} -3.1888 & 2.6065 & 0.7159 & 1.5667 \\ -2.1273 & 2.7201 & -0.0887 & 1.0648 \end{bmatrix},$$

$$K_2 = \begin{bmatrix} -1.3886 & 6.8116 & 1.1032 & 2.8949 \\ -1.1547 & 7.2332 & -0.0831 & 2.3852 \end{bmatrix},$$

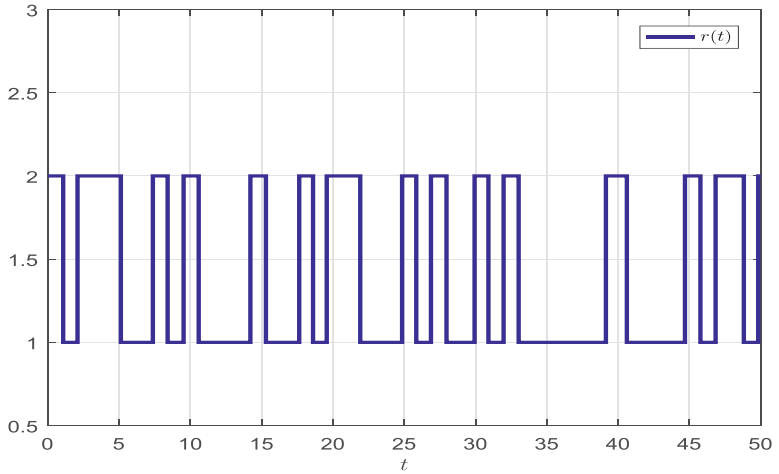

Fig. 9. The switching signal of Example 2.

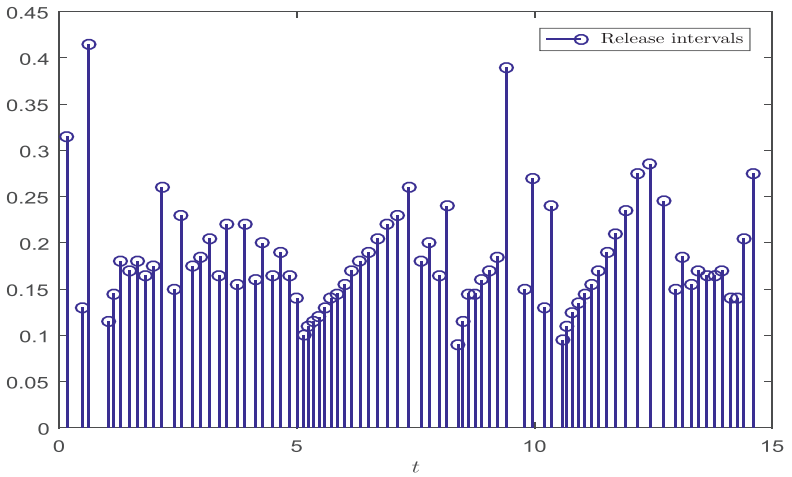

Fig. 10. Release intervals and instants of the MDSETM in Case 1 of Example 2.

$$\Lambda_1 = \begin{bmatrix} 4.1716 & -0.7630 & 0.3935 & -0.1378 \\ -0.7630 & 4.6068 & -0.1280 & 0.5114 \\ 0.3935 & -0.1280 & 0.0850 & -0.0056 \\ -0.1378 & 0.5114 & -0.0056 & 0.0884 \end{bmatrix},$$

$$\Lambda_2 = \begin{bmatrix} 2.8756 & -0.3917 & 0.2977 & -0.0522 \\ -0.3917 & 4.1015 & -0.0951 & 0.4533 \\ 0.2977 & -0.0951 & 0.0770 & -0.0000 \\ -0.0522 & 0.4533 & -0.0000 & 0.0784 \end{bmatrix}.$$

Figure 10 illustrates the event-triggered release intervals and instants under the presented MDSETM-based controller. Figure 11 describes the state trajectories under control input. It is clear that the SCLS achieves stability. Table 4 shows a comparison results of the NTEs under different ETMs. It can be found the NTEs under the MDSETM is 72% less than that under the PSM in [45], 65% less than that under the STEM in [29], and 5% less than that under the STEM in [44].

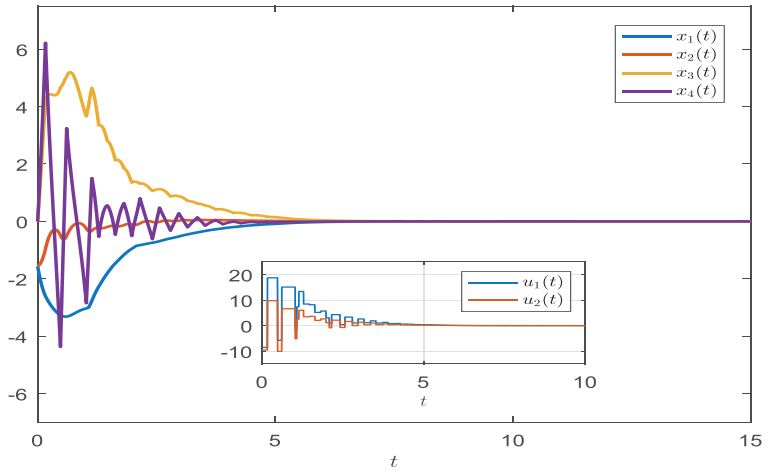

Fig. 11. State trajectories with control in Case 1 of Example 2.

Table 4
Comparison of the NTEs under different ETMs in Case 1 of Example 2.

Mechanism	The NTEs	Transmission rate (%)
PSM in [45]	300	100
STEM in [29]	280	93
STEM in [44]	100	33
MDSETM	83	28

Case 2. $(\mathscr{Q}, \mathscr{S}, \mathscr{R})$ **- dissipative performances**

Choose $\Upsilon_1 = -I$, $\Upsilon_2 = I$, $\Upsilon_3 = 6.5I$, and $\Upsilon_4 = 0$. Then, by solving LMIs (30)–(34) in Theorem 2 via the SeDuMi solver under the YALMIP interface in MATLAB, we can obtain

$$K_1 = \begin{bmatrix} -3.0617 & 2.0128 & 0.4705 & 0.9671 \\ -2.2326 & 2.2161 & -0.1472 & 0.6039 \end{bmatrix},$$

$$\Lambda_1 = \begin{bmatrix} 302.9519 & -41.1912 & 49.8130 & -14.6950 \\ -41.1912 & 100.2976 & -12.0190 & 19.8871 \\ 49.8130 & -12.0190 & 13.4775 & -1.0957 \\ -14.6950 & 19.8871 & -1.0957 & 6.0689 \end{bmatrix},$$

$$K_2 = \begin{bmatrix} 0.4235 & 5.2170 & 1.2512 & 1.5890 \\ -0.7165 & 5.9327 & 0.1389 & 1.3564 \end{bmatrix},$$

$$\Lambda_2 = \begin{bmatrix} 247.3384 & -24.1746 & 48.2814 & -6.8041 \\ -24.1746 & 119.5976 & -12.7310 & 22.4193 \\ 48.2814 & -12.7310 & 13.1804 & -1.5809 \\ -6.8041 & 22.4193 & -1.5809 & 5.5608 \end{bmatrix}.$$

Figure 12 illustrates the event-triggered release intervals and instants under the designed MDSETM-based controller. Figure 13 describes the state trajectories under control input. Obviously, the SCLS quickly achieves stability. Hence, the simulations validate of the proposed control method. Table 5 shows a comparison results of the NTEs under different ETMs. We can see that the NTEs under the MDSETM is 51% less than that under the PSM in [45], 45% less than that under the STEM in [29], and 3% less than that under the STEM in [44].

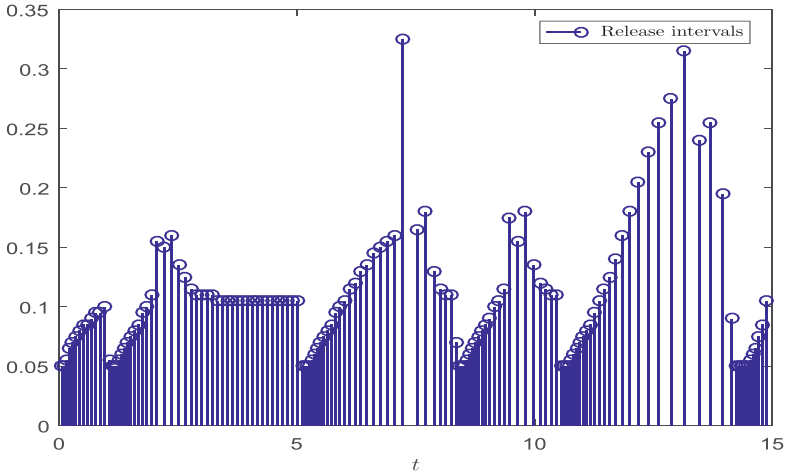

Fig. 12. Release intervals and instants of the MDSETM in Case 2 of Example 2.

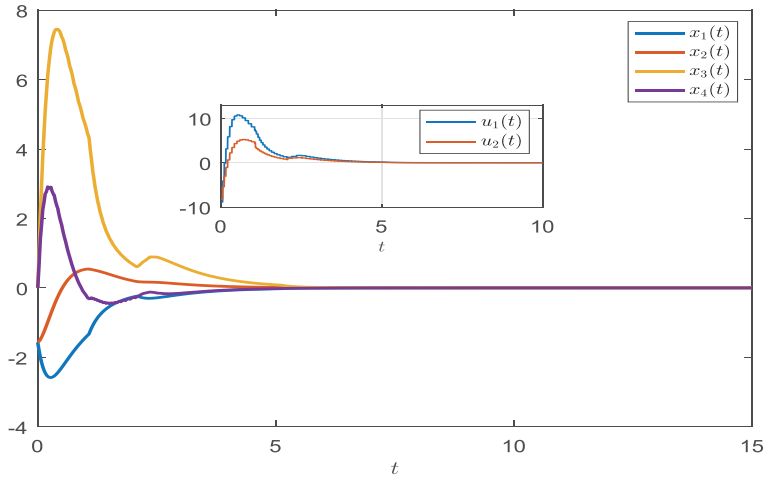

Fig. 13. State trajectories with control in Case 2 of Example 2.

Table 5
Comparison of the NTEs under different ETMs in Case 2 of Example 2.

Mechanism	The NTEs	Transmission rate (%)
PSM in [45]	300	100
STEM in [29]	281	94
STEM in [44]	157	52
MDSETM	147	49

5. Conclusion

The paper has addressed the extended stabilization problem for uncertain semi-MSSs with disturbances. A MDSETM has been devised to determine the triggered moments by introducing the mode-dependent event-triggered matrix and disturbance related term into the threshold function. By employing time- and mode-dependent piecewise-defined $V(t)$, a criterion for stochastic stability and extended dissipativity of semi-MSS (6) has been proposed in Theorem 1. On the basis of the criterion, a LMIs-based co-design of needed feedback-gain and event-triggered matrices has been developed in Theorem 2 via using some equivalent transformations of matrix inequalities. Finally, a DC motor model and 2-DOF robot arm model have been employed to illustrate the advantages of the MDSETM and validity of the proposed controller design method.

In this paper, the designed MDSETM is based on measurable disturbances. In the case when the disturbances are unmeasurable, one may first obtain the estimate of these disturbances via designing observer, and then use them in the ETM. This will be one of the directions of our future research.

Declaration of Competing Interest

The authors declare that they have no conflict of interest.

Data availability

No data was used for the research described in the article.

Acknowledgment

This work was supported by the Key Research and Development Project of Anhui Province (Grant No. 202004a07020028) and the Natural Science Foundation of the Anhui Higher Education Institutions (Grant No. 2022AH050290).

References

[1] O.L.V. Costa, M.D. Fragoso, M.G. Todorov, Continuous-Time Markov Jump Linear Systems, Springer, 2012.
[2] P. Shi, Y. Yin, F. Liu, J. Zhang, Robust control on saturated Markov jump systems with missing information, Inf. Sci. 265 (2014) 123–138.
[3] R. Sakthivel, M. Rathika, S. Santra, M. Muslim, Observer-based dissipative control for Markovian jump systems via delta operators, Int. J. Syst. Sci. 48 (2017) 247–256.
[4] H. He, W. Qi, Z. Liu, M. Wang, Adaptive attack-resilient control for Markov jump system with additive attacks, Nonlinear Dyn. 103 (2021) 1585–1598.
[5] D. Zhai, L. An, J. Li, Q. Zhang, Fault detection for stochastic parameter-varying Markovian jump systems with application to networked control systems, Appl. Math. Modell. 40 (2016) 2368–2383.
[6] Z. Cao, Y. Niu, Finite-time sliding mode control of Markovian jump systems subject to actuator nonlinearities and its application to wheeled mobile manipulator, J. Franklin Inst. 355 (2018) 7865–7894.
[7] J. Cheng, Y. Wu, H. Yan, Z.G. Wu, K. Shi, Protocol-based filtering for fuzzy Markov affine systems with switching chain, Automatica 141 (2022) 110321.
[8] L. Zhang, T. Yang, P. Colaneri, Stability and stabilization of semi-Markov jump linear systems with exponentially modulated periodic distributions of sojourn time, IEEE Trans. Autom. Control 62 (2016) 2870–2885.
[9] S. Ouaret, Production control problem with semi-Markov jump under stochastic demands and deteriorating inventories, Appl. Math. Modell. 107 (2022) 85–102.
[10] J. Zhou, Y. Liu, J. Xia, Z. Wang, S. Arik, Resilient fault-tolerant anti-synchronization for stochastic delayed reaction–diffusion neural networks with semi-Markov jump parameters, Neural Netw. 125 (2020) 194–204.
[11] J. Yang, Z. Ning, Y. Zhu, L. Zhang, H.K. Lam, Semi-Markov jump linear systems with bi-boundary sojourn time: anti-modal-asynchrony control, Automatica 140 (2022) 110270.
[12] M. Gao, W. Qi, J. Cao, J. Cheng, K. Shi, Y. Gao, SMC for phase-type stochastic nonlinear semi-Markov jump systems, Nonlinear Dyn. 108 (2022) 279–292.
[13] S. Dong, G. Chen, M. Liu, Z.G. Wu, Robust adaptive $\mathscr{H}_\infty$ control for networked uncertain semi-Markov jump nonlinear systems with input quantization, Sci. China Inf. Sci. 65 (2022) 189201.
[14] H. Shen, F. Li, S. Xu, V. Sreeram, Slow state variables feedback stabilization for semi-Markov jump systems with singular perturbations, IEEE Trans. Autom. Control 63 (2017) 2709–2714.
[15] E.K. Boukas, Z. Liu, G. Liu, Delay-dependent robust stability and $\mathscr{H}_\infty$ control of jump linear systems with time-delay, Int. J. Control 74 (2001) 329–340.
[16] Z. Xu, H. Su, P. Shi, Z. Wu, Asynchronous $\mathscr{H}_\infty$ control of semi-Markov jump linear systems, Appl. Math. Comput. 349 (2019) 270–280.
[17] J. Zhang, S. Ma, Robust $\mathscr{H}_\infty$ indefinite guaranteed cost dynamic output feedback control of singular semi-markov jump systems, J. Frankl. Inst. (2021), doi:10.1016/j.jfranklin.2021.04.051.
[18] Y. Xu, J. Li, R. Lu, C. Liu, Y. Wu, Finite-horizon $\mathscr{L}_2 - \mathscr{L}_\infty$ synchronization for time-varying Markovian jump neural networks under mixed-type attacks: observer-based case, IEEE Trans. Neural Netw. Learn. Syst. 30 (2018) 1695–1704.
[19] Z. Yan, C. Sang, M. Fang, J. Zhou, Energy-to-peak consensus for multi-agent systems with stochastic disturbances and Markovian switching topologies, Trans. Inst. Meas. Control. 40 (2018) 4358–4368.
[20] S. He, F. Liu, $\mathscr{L}_2 - \mathscr{L}_\infty$ fuzzy control for Markov jump systems with neutral time-delays, Math. Comput. Simul. 92 (2013) 1–13.
[21] X. Hu, J. Xia, Y. Wei, B. Meng, H. Shen, Passivity-based state synchronization for semi-Markov jump coupled chaotic neural networks with randomly occurring time delays, Appl. Math. Comput. 361 (2019) 32–41.
[22] B. Zhang, W.X. Zheng, S. Xu, Filtering of Markovian jump delay systems based on a new performance index, IEEE Trans. Circuits Syst. I Regular Papers 60 (2013) 1250–1263.
[23] R. Sakthivel, A. Parivallal, N.H. Tuan, S. Manickavalli, Nonfragile control design for consensus of semi-Markov jumping multiagent systems with disturbances, Int. J. Adapt. Control Signal Process 35 (2021) 1039–1061.
[24] W. Chen, M.-Z. Dai, C. Guan, Z. Fei, Extended dissipativity of semi-Markov jump neural networks with partly unknown transition rates, Neurocomputing 423 (2021) 601–608.
[25] K. Ding, Q. Zhu, Extended dissipative anti-disturbance control for delayed switched singular semi-Markovian jump systems with multi-disturbance via disturbance observer, Automatica 128 (2021) 109556.
[26] C. Pradeep, Y. Cao, R. Murugesu, R. Rakkiyappan, An event-triggered synchronization of semi-Markov jump neural networks with time-varying delays based on generalized free-weighting-matrix approach, Math. Comput. Simulat. 155 (2019) 41–56.
[27] P. Tabuada, Event-triggered real-time scheduling of stabilizing control tasks, IEEE Trans. Autom. Control 52 (2007) 1680–1685.
[28] W.H. Heemels, M. Donkers, A.R. Teel, Periodic event-triggered control for linear systems, IEEE Trans. Autom. Control 58 (2012) 847–861.
[29] A. Selivanov, E. Fridman, Event-triggered $\mathscr{H}_\infty$ control: aswitching approach, IEEE Trans. Autom. Control 61 (2016) 3221–3226.
[30] Z. Fei, C. Guan, H. Gao, Exponential synchronization of networked chaotic delayed neural network by a hybrid event trigger scheme, IEEE Trans. Neural Netw. Learn. Syst. 29 (2017) 2558–2567.
[31] S. Ding, Z. Wang, Event-triggered synchronization of discrete-time neural networks: a switching approach, Neural Netw. 125 (2020) 31–40.
[32] X. Wang, Z. Wang, Q. Song, H. Shen, X. Huang, A waiting-time-based event-triggered scheme for stabilization of complex-valued neural networks, Neural Netw. 121 (2020) 329–338.
[33] Z. Yan, X. Huang, Y. Fan, J. Xia, H. Shen, Threshold-function-dependent quasi-synchronization of delayed memristive neural networks via hybrid event-triggered control, IEEE Trans. Syst. Man Cybern. Syst. 51 (2021) 6712–6722.
[34] X. Liu, X. Yu, X. Zhou, H. Xi, Finite-time $\mathscr{H}_\infty$ control for linear systems with semi-Markovian switching, Nonlinear Dyn. 85 (2016) 2297–2308.
[35] W. Qi, G. Zong, W. Zheng, Adaptive event-triggered SMC for stochastic switching systems with semi-Markov process and application to boost converter circuit model, IEEE Trans. Circuits Syst. I Regular Papers 68 (2021) 786–796.
[36] A. Vargas, E. Costa, J. do Val, On the control of Markov jump linear systems with no mode observation: application to a DC motor device, Int. J. Robust Nonlinear Control 23 (2013) 1136–1150.
[37] Y. Yin, P. Shi, F. Liu, C. Lim, Robust control for nonhomogeneous Markov jump processes: an application to DC motor device, J. Frankl. Inst. 351 (2014) 3322–3338.

[38] X. Yao, L. Zhang, W. Zheng, Uncertain disturbance rejection and attenuation for semi-Markov jump systems with application to 2-degree-freedom robot arm, IEEE Trans. Circuits Syst. I Regular Papers 68 (2021) 3836–3845.
[39] C. Du, C. Yang, F. Li, W. Gui, A novel asynchronous control for artificial delayed Markovian jump systems via output feedback sliding mode approach, IEEE Trans. Syst. Man. Cybern. Syst. 49 (2018) 364–374.
[40] I. Wolf, D. Munoz, W. Marquardt, Consistent hierarchical economic NMPC for a class of hybrid systems using neighboring-extremal updates, J. Process Control 24 (2014) 389–398.
[41] T.H. Lee, J.H. Park, S.M. Lee, O.M. Kwon, Robust synchronisation of chaotic systems with randomly occurring uncertainties via stochastic sampled-data control, Int. J. Control 86 (2013) 107–119.
[42] X. Chang, J. Song, X. Zhao, Resilient h_∞ filter design for continuous-time nonlinear systems, IEEE Trans. Fuzzy Syst. 30 (2022) 591–596.
[43] J. Zhou, S. Xu, B. Zhang, Y. Zou, H. Shen, Robust exponential stability of uncertain stochastic neural networks with distributed delays and reaction-diffusions, IEEE Trans. Neural Netw. Learn. Syst. 23 (2012) 1407–1416.
[44] W. Wu, L. He, J. Zhou, Z. Xuan, S. Arik, Disturbance-term-based switching event-triggered synchronization control of chaotic Lurie systems subject to a joint performance guarantee, Commun. Nonlinear Sci. Numer. Simulat. 115 (2022) 106774.
[45] C. Hua, C. Ge, X. Guan, Synchronization of chaotic Lur'e systems with time delays using sampled-data control, IEEE Trans. Neural Netw. Learn. Syst. 26 (2014) 1214–1221.
[46] J. Huang, Y. Shi, Stochastic stability and robust stabilization of semi-Markov jump linear systems, Int. J. Robust Nonlinear Control 23 (2013) 2028–2043.
[47] K. Gu, J. Chen, V.L. Kharitonov, Stability of Time-Delay Systems, Springer Science & Business Media, 2003.
[48] Z. Zhang, J. Zhang, Z. Ai, A novel stability criterion of the time-lag fractional-order gene regulatory network system for stability analysis, Commun. Nonlinear Sci. Numer. Simulat. 66 (2019) 96–108.
[49] L. Xie, M. Fu, C.E. de Souza, et al., $\mathscr{H}_\infty$ control and quadratic stabilization of systems with parameter uncertainty via output feedback, IEEE Trans. Autom. Control 37 (1992) 1253–1256.
[50] J. Wang, X. Zhang, Q. Han, Event-triggered generalized dissipativity filtering for neural networks with time-varying delays, IEEE Trans. Neural Netw. Learn. Syst. 27 (2016) 77–88.
[51] Y. Liu, F. Fang, J. Park, H. Kim, X. Yi, Asynchronous output feedback dissipative control of Markovian jump systems with input time delay and quantized measurements, Nonlinear Anal. Hybri. Syst. 31 (2019) 109–122.
[52] X. Zhang, Q. Han, X. Ge, B. Zhang, Delay-variation-dependent criteria on extended dissipativity for discrete-time neural networks with time-varying delay, IEEE Trans. Neural Netw. Learn. Syst. (2021), doi:10.1109/TNNLS.2021.3105591. Online
[53] Z. Feng, J. Lam, Robust reliable dissipative filtering for discrete delay singular systems, Signal Process. 92 (2012) 3010–3025.
[54] Z. Wu, P. Shi, H. Su, J. Chu, Sampled-data synchronization of chaotic Lur'e systems with time delays, IEEE Trans. Neural Netw. Learn. Syst. 24 (2013) 410–421.